

Supporting Information – SI for

On the Redox Series of Cyclometalated Nickel Complexes $[\text{Ni}((\text{R})\text{Ph}(\text{R}')\text{bpy})\text{Br}]^{+/0/-2-}$ ($\text{H}-(\text{R})\text{Ph}(\text{R}')\text{bpy}$ = substituted 6-phenyl-2,2'-bipyridines)

Aaron Sandleben^a, Nicolas Vogt^a, Gerald Hörner^{b,*}, and Axel Klein^{a,*}

^a Universität zu Köln, Department für Chemie, Institut für Anorganische Chemie, Greinstraße 6, D-50939 Köln, Germany

^b Institut für Chemie, Theoretische Chemie, Technische Universität Berlin, Straße des 17. Juni 135, D-10623 Berlin, Germany

* to whom the correspondence should be addressed: e-mail: axel.klein@uni-koeln.de

Contents:

A Syntheses **S2 to S5**

B Supporting Figures (Figures S1 to S31) **S6 to S21**

Figure S1. TG-DTA measurements of $[\text{Ni}(\text{Ph}(7-\text{CH}_3)\text{bpy})\text{Br}]$ and $[\text{Ni}((\text{MeO})\text{Phbpy})\text{Br}]$.

Figure S2. TG-DTA measurements of $[\text{Ni}(\text{Ph}(7-\{3-\text{MeOPh}\})\text{bpy})\text{Br}]$ and $[\text{Ni}(\text{Ph}(7-\text{CF}_3)\text{bpy})\text{Br}]$.

Figure S3. TG-DTA measurement of $[\text{Ni}(\text{Ph}(6-\{2-\text{CH}_3\text{Ph}\})\text{bpy})\text{Br}]$.

Figure S4. Powder XRD of $[\text{Ni}((\text{MeO})\text{Ph}(7-\text{CF}_3)\text{bpy})\text{Br}]$, $[\text{Ni}(\text{Ph}(7-\{3-\text{MeOPh}\})\text{bpy})\text{Br}]$, $[\text{Ni}(\text{Ph}(7-\text{CH}_3)\text{bpy})\text{Br}]$, $[\text{Ni}(\text{Ph}(6-\{4-\text{MeOPh}\})\text{bpy})\text{Br}]$, and $[\text{Ni}((\text{MeO})\text{Phbpy})\text{Br}]$.

Figure S5. Powder XRD of $[\text{Ni}(\text{Ph}(6-\{2-\text{CH}_3\text{Ph}\})\text{bpy})\text{Br}]$ together with simulated data from single crystal data.

Figure S6. Powder XRD of $[\text{Ni}(\text{Ph}(7-\text{CF}_3)\text{bpy})\text{Br}]$ together with simulated data from single crystal data.

Figure S7. Molecular structure and crystal structure of $\text{H}-(\text{MeO})\text{Phbpy}$.

Figure S8. Crystal structures of $\text{Br}-\text{Ph}(7-\text{CF}_3)\text{bpy}$ and $\text{H}-\text{Ph}(7-\text{CF}_3)\text{bpy}$.

Figure S9. Molecular structures of $\text{Br}-\text{Ph}(7-\text{CF}_3)\text{bpy}$ and $\text{H}-\text{Ph}(7-\text{CF}_3)\text{bpy}$.

Figure S10. Molecular structure and crystal structure of $\text{Br}-\text{PhTriazPy}$.

Figure S11. Molecular structure and crystal structure of $\text{Br}-(\text{MeO})\text{PhTriazPy}$.

Figure S12. Molecular structure and crystal structure of $[\text{Ni}(\text{Ph}(7-\text{CF}_3)\text{bpy})\text{Br}]$.

Figure S13. Molecular structure and crystal structure of $[\text{Ni}(\text{Ph}(6-\{2-\text{CH}_3\text{Ph}\})\text{bpy})\text{Br}]$.

Figure S14. Molecular structure and crystal structure of $[\text{Ni}(\text{Ph}(7-\{3-\text{MeOPh}\})\text{bpy})\text{Br}]$.

Figure S15. Molecular structure and crystal structure of $[\text{Ni}(\text{Ph}(6-\{4-\text{MeOPh}\})\text{bpy})\text{Br}]$.

Figure S16. ^1H NMR spectrum of $[\text{Ni}(\text{Ph}(7-\text{CF}_3)\text{bpy})\text{Br}]$ in CD_2Cl_2 at 600 MHz.

Figure S17. ^1H NMR spectrum of $[\text{Ni}(\text{Ph}(7-\text{CH}_3)\text{bpy})\text{Br}]$ in CDCl_3 at 300 MHz.

Figure S18. ^1H NMR spectrum of $[\text{Ni}(\text{Ph}(6-\{2-\text{CH}_3\text{Ph}\})\text{bpy})\text{Br}]$ in CDCl_3 at 300 MHz.

Figure S19. Absorption spectra of the complexes $[\text{Ni}((\text{R})\text{Ph}(\text{R}')\text{bpy})\text{Br}]$ in THF.

Figure S20. Selected DFT calculated skeletal vibrational modes of $[\text{Ni}(\text{Phbpy})\text{Br}]^{+-}$.

Figure S21. DFT calculated composition of the SOMO of $[\text{Ni}((\text{MeO})\text{Phbpy})\text{Br}]^{+-}$ and $[\text{Ni}(\text{Ph}(7-\text{CF}_3)\text{bpy})\text{Br}]^{+-}$.

Figure S22. DFT calculated UV-vis absorptions of $[\text{Ni}(\text{III})(\text{MeO})\text{Phbpy})\text{Br}]^{+-}$.

Figure S23. Absorption spectrum recorded after the reaction of $\text{Ni}(\text{BF}_4)_2$ with $\text{H}-(\text{MeO})\text{Phbpy}$ in THF.

Figure S24. UV-vis spectra of $[\text{Ni}(\text{Ph}(7-\text{CF}_3)\text{bpy})\text{Br}]$ during electrochemical oxidation and reduction.

Figure S25. UV-vis spectra of $[\text{Ni}(\text{Ph}(7-\text{CH}_3)\text{bpy})\text{Br}]$ during electrochemical oxidation and reduction.

Figure S26. UV-vis spectra of $[\text{Ni}((\text{MeO})\text{Ph}(7-\text{CF}_3)\text{bpy})\text{Br}]$ during electrochemical oxidation and reduction.

Figure S27. UV-vis spectra of $[\text{Ni}((\text{MeO})\text{Ph}(7-\text{CH}_3)\text{bpy})\text{Br}]$ during electrochemical oxidation and reduction.

Figure S28. X Band EPR spectrum during electrochemical reduction of $\text{H}-\text{Phbpy}$.

Figure S29. X Band EPR spectrum during electrochemical reduction of $[\text{Ni}(\text{Ph}(6-\{2-\text{CH}_3\text{Ph}\})\text{bpy})\text{Br}]$ at rt.

Figure S30. X Band EPR spectrum during electrochemical reduction of $[\text{Ni}(\text{Ph}(6-\{2-\text{CH}_3\text{Ph}\})\text{bpy})\text{Br}]$ at 110 K.

Figure S31. Cyclovoltammograms of $[\text{Ni}((\text{MeO})\text{Phbpy})\text{Br}]$ and $[\text{Ni}(\text{Ph}(7-\text{CF}_3)\text{bpy})\text{Br}]$.

C Supporting Tables (Tables S1 to S11) **S22 to S26**

Table S1. Electrochemical data for the complexes $[\text{Ni}((\text{R})\text{Ph}(\text{R}')\text{bpy})\text{Br}]$.

Table S2. Absorption maxima of the protoligands $\text{Br}-(\text{R})\text{Ph}(\text{R}')\text{bpy}$.

Table S3. Electrochemical data for the protoligands $\text{H}-(\text{R})\text{Ph}(\text{R}')\text{bpy}$ and $\text{Br}-(\text{R})\text{Ph}(\text{R}')\text{bpy}$.

Table S4. Data from structure solution and refinement for complexes $[\text{Ni}((\text{MeO})\text{Phbpy})\text{Br}]$, $[\text{Ni}(\text{Ph}(7-\{\text{3-MeOPh}\})\text{bpy})\text{Br}]$, and $[\text{Ni}(\text{Ph}(6-\{\text{4-MeOPh}\})\text{bpy})\text{Br}]$.

Table S5. Data from structure solution and refinement for complexes $[\text{Ni}(\text{Ph}(7-\text{CF}_3)\text{bpy})\text{Br}]$ and $[\text{Ni}(\text{Ph}(6-\{\text{2-CH}_3\text{Ph}\})\text{bpy})\text{Br}]$.

Table S6. Data from structure solution and refinement for compounds $\text{Br}-\text{PhTriazPy}$, $\text{Br}-(\text{MeO})\text{PhTriazPy}$, $\text{H}-(\text{MeO})\text{Phbpy}$, $\text{H}-\text{Ph}(7-\text{CF}_3)\text{bpy}$, and $\text{Br}-\text{Ph}(7-\text{CF}_3)\text{bpy}$.

Table S7. Selected DFT calculated and experimental structural data for complexes $[\text{Ni}(\text{Ph}(7-\text{CF}_3)\text{bpy})\text{Br}]$ and $[\text{Ni}(\text{Ph}(6-\{\text{2-CH}_3\text{Ph}\})\text{bpy})\text{Br}]$.

Table S8. Selected DFT calculated structural data for complexes $[\text{Ni}((\text{R})\text{Ph}(\text{R}')\text{bpy})\text{Br}]$.

Table S9. DFT calculated low-energy transitions for $[\text{Ni}((\text{R})\text{Ph}(\text{R}')\text{bpy})\text{Br}]$.

Table S10. DFT calculated low-energy transitions for $[\text{Ni}(\text{III})(\text{MeO})\text{Phbpy})\text{Br}]^{++}$.

Table S11. DFT calculated EPR parameters for $[\text{Ni}((\text{R})\text{Ph}(\text{R}')\text{bpy})\text{Br}]^-$.

A Syntheses:

Synthesis of the Kröhnke reagent *N*-(1-(2-Pyridinyl)-1-oxo-2-ethyl)pyridiniumiodide: 2-Acetylpyridine (6.06 g, 50 mmol, 1 eq.) and iodine (6.35 g, 50 mmol, 1 eq.) were refluxed in 50 mL of pyridine for 1 h. After cooling to ambient temperature the reaction mixture was filtered and the resulting precipitate was washed with pyridine and acetone and dried in vacuum. Yield: 12.9 g, 39.5 mmol, 79%. ^1H NMR (300 MHz, DMSO-d₆) δ = 9.00 (d, 2H, $^3J_{HH}$ = 5.2 Hz), 8.87 (d, 1H, $^3J_{HH}$ = 4.5 Hz), 8.72 (t, 1H, $^3J_{HH}$ = 7.8 Hz), 8.27 (dd, 2H, $^3J_{HH}$ = 7.9, $^3J_{HH}$ = 6.6 Hz), 8.10–8.02 (m, 2H), 7.83 (ddd, 1H, $^3J_{HH}$ = 7.4, $^4J_{HH}$ = 4.8, $^5J_{HH}$ = 1.6 Hz), 6.50 (s, 2H) ppm.

Synthesis of Mannich adducts - general procedure: Dimethylamine hydrochloride (7.80 g, 95.6 mmol, 1.30 eq.), paraformaldehyde (2.94 g, 97.8 mmol, 1.33 eq.) and the corresponding acetophenone derivative (73.5 mmol, 1 eq.) were suspended in 40 mL of ethanol. After addition of 2 mL conc. HCl the mixture was heated to reflux for 20 h and then cooled to ambient temperature. The solution was diluted with 150 mL of acetone and kept at -18 °C for 7-20 h. The white crystalline precipitate was filtered off, washed with acetone and dried in vacuum.

1-(2-Bromophenyl)-3-(dimethylamino)propan-1-one hydrochloride: Starting material: 14.63 g 2'-bromoacetophenone. Colorless crystals. Yield: 10.9 g, 37.1 mmol, 50%. ^1H NMR (300 MHz, CD₂Cl₂) δ = 7.71–7.56 (m, 2H), 7.51–7.31 (m, 2H), 3.67 (t, 2H, $^3J_{HH}$ = 6.8 Hz), 3.46 (t, 2H, $^3J_{HH}$ = 6.8 Hz), 2.81 (s, 6H) ppm.

1-(3-Methoxyphenyl)-3-(dimethylamino)propan-1-one hydrochloride: Starting material: 11.04 g 3'-methoxyacetophenone. Colorless crystals. Yield: 15.4 g, 63.2 mmol, 86%. ^1H NMR (300 MHz, CDCl₃) δ = 7.58 (d, 1H, $^3J_{HH}$ = 7.9 Hz), 7.51–7.32 (m, 2H), 7.19–7.10 (m, 1H), 3.85 (s, 3H), 3.73 (t, 2H, $^3J_{HH}$ = 6.9 Hz), 3.51 (t, 2H, $^3J_{HH}$ = 6.9 Hz), 2.85 (s, 6H) ppm.

Synthesis of Chalkone derivatives – general procedure: 2'-Bromoacetophenone (3.98 g, 20.0 mmol, 1 eq.) and sodium hydroxide (1.14 g, 28.5 mmol, 1.4 eq.) were dissolved in H₂O/EtOH (20 mL/20 mL) and cooled to 0 °C. Then the corresponding aldehyde (20.0 mmol, 1 eq) was added and the reaction was stirred for 12-24 h at ambient temperature. The off-white precipitate was filtered off and recrystallized from ethanol.

1-(2-Bromophenyl)-3-(3-nitrophenyl)-prop-2-en-1-on: Starting material: 3.02 g 3-nitrobenzaldehyde. Off white powder. Yield: 4.3 g, 12.8 mmol, 64%. ^1H NMR (300 MHz, acetone-d₆) δ = 8.60 (t, 1H, $^4J_{HH}$ = 2.0 Hz), 8.36–8.18 (m, 2H), 7.84–7.70 (m, 2H), 7.69–7.37 (m, 5H) ppm.

1-(2-Bromophenyl)-3-(2-methylphenyl)-prop-2-en-1-on: Starting material: 2.40 g 2-methylbenzaldehyde. Colorless powder. Yield: 4.2 g, 13.8 mmol, 69%. ^1H NMR (300 MHz, CDCl₃) δ = 7.61 (m, 3H), 7.24 (m, 6H), 6.92 (d, 1H, $^3J_{HH}$ = 16.0 Hz), 2.27 (s, 3H) ppm. ^{13}C NMR (75 MHz, CDCl₃) δ = 194.7, 144.2, 144.2, 141.4, 138.4, 133.9, 133.4, 131.5, 131.0, 130.7, 129.4, 127.5, 127.0, 126.7, 126.6, 119.6, 19.8 ppm.

Synthesis of Pyridinehydrazoneamide: 2-Cyanopyridine (15 mL, 155.8 mmol, 1 eq.) and hydrazine hydrate (10 mL, 160.5 mmol, 1 eq.) were mixed and ethanol was added until the solution was clear (10 mL). The mixture was stirred at ambient temperature for 16 h and the product precipitated as a yellow solid. The product was filtered off and washed with diethyl ether. Yellow crystals. Yield: 15.67 g, 115.3 mmol, 74%. ^1H NMR (300 MHz, CD₂Cl₂) δ = 8.50 (d, 1H, $^3J_{HH}$ = 4.8 Hz), 8.00 (d, 1H, $^3J_{HH}$ = 8.1 Hz), 7.69 (td, 1H, $^3J_{HH}$ = 7.8, $^4J_{HH}$ =

1.7 Hz), 7.26 (ddd, 1H, $^3J_{HH} = 7.4$, $^4J_{HH} = 4.9$, $^5J_{HH} = 1.1$ Hz), 5.05 (s, 2H), 4.36 (s, 2H) ppm. ^{13}C NMR (75 MHz, CD_2Cl_2) $\delta = 151.64$, 148.45, 136.83, 124.16, 120.06, 105.56 ppm.^[1]

Synthesis of R-Phenylglyoxal hydrate - general procedure: Selenium dioxide (4.94 g, 44.5 mmol, 1 eq.) was dissolved in 50 mL dioxane and 5 mL of water at 55 °C. After that, R-acetophenone (44.5 mmol, 1 eq.) was added and refluxed for 24 h. After cooling to ambient temperature the mixture was filtered over silicagel and Celite and the solvent was removed to give the raw product as yellow/orange oil. The raw products can be used in the next reactions without further purification.^[2]

3-Methoxyphenylglyoxal hydrate: Starting material: 6.68 g 3'-methoxyacetophenone. Pure product was obtained as yellowish powder by column chromatography (2:1 *c*-hexane/acetone) in low yield of 12%. ^1H NMR (300 MHz, CDCl_3) $\delta = 9.67$ (s, "1H"), 7.74 (dt, 1H, $^3J_{HH} = 7.7$, $^5J_{HH} = 1.2$ Hz), 7.63 (dd, 1H, $^4J_{HH} = 2.7$, $^5J_{HH} = 1.5$ Hz), 7.39 (t, 1H, $^3J_{HH} = 8.0$ Hz), 7.22–7.11 (m, 1H), 6.34 (d, 1H, $^3J_{HH} = 10.4$ Hz), 5.01 (d, 1H, $^3J_{HH} = 10.4$ Hz) ppm.

2-Bromophenylglyoxal hydrate: Used starting material: 8.86 g 2'-bromoacetophenone. The crude product was used without further purification.

Syntheses of 5-(R-Phenyl)-3-(2-pyridinyl)-1,2,4-triazine - general procedure: The corresponding R-phenylglyoxal hydrate (approx. 30.0 mmol, 1 eq.) and pyridinehydrazoneamide (4.08 g, 30.0 mmol, 1 eq.) were dissolved in 100 mL ethanol and heated under reflux for 22 h. While cooling to ambient temperature the product precipitated as a yellow solid, was filtered off and washed with cold ethanol and diethyl ether. In case of high amounts of impurities it was dissolved in ethanol and filtered over Celite and recrystallized from diethyl ether.^[3]

5-(2-Bromophenyl)-3-(2-pyridinyl)-1,2,4-triazine (Br-PhTriazPy): Yellow crystals. Yield: 6.4 g, 20.4 mmol, 68%. ^1H NMR (300 MHz, CDCl_3) $\delta = 9.68$ (s, 1H), 8.92 (d, 1H, $^3J_{HH} = 5.6$ Hz), 8.69 (d, 1H, $^3J_{HH} = 7.9$ Hz), 7.93 (td, 1H, $^3J_{HH} = 7.8$, $^4J_{HH} = 1.8$ Hz), 7.77 (td, 2H, $^3J_{HH} = 7.8$, $^4J_{HH} = 1.4$ Hz), 7.57–7.46 (m, 2H), 7.46–7.37 (m, 1H) ppm.

5-(3-Methoxyphenyl)-3-(2-pyridinyl)-1,2,4-triazine (H-(MeO)PhTriazPy): Yellow crystals. Yield: 3.6 g, 13.8 mmol, 46%. ^1H NMR (300 MHz, CDCl_3) $\delta = 9.68$ (s, 1H), 8.93 (d, 1H, $^3J_{HH} = 3.9$ Hz), 8.65 (d, 1H, $^3J_{HH} = 7.9$ Hz), 7.93 (td, 1H, $^3J_{HH} = 7.8$, $^4J_{HH} = 1.8$ Hz), 7.89–7.81 (m, 2H), 7.55–7.46 (m, 2H), 7.20–7.12 (m, 1H), 3.94 (s, 3H) ppm.

Syntheses of Br-Ph(R')bpy from triazines – general procedure: Sodiumhydroxid (0.38 g, 9.6 mmol, 3 eq.) was dissolved in 40 mL ethanol. Slowly the respective acetyl derivative (6.4 mmol, 2 eq.) dissolved in 10 mL ethanol was added. After 15 min 5-(2-bromophenyl)-3-(2-pyridinyl)-1,2,4-triazine (1.00 g, 3.2 mmol, 1 eq) or 5-(2-bromo-5-methoxyphenyl)-3-(2-pyridinyl)-1,2,4-triazine (1.10 g, 3.2 mmol, 1 eq) respectively was added and the reaction mixture was refluxed for 24 h. After cooling to ambient temperature 13 mL of 2 M HCl ($\text{H}_2\text{O}/\text{conc. HCl}$, 5/1) were added and stirred for 1 h. The solution was brought to pH 9 with saturated $\text{Na}_2\text{CO}_3/\text{H}_2\text{O}$ solution and was extracted twice with CH_2Cl_2 . The organic phases were washed with water and dried over MgSO_4 . The solvent was evaporated to give the crude product.^[4]

6-(2-Bromophenyl)-4-(4-methoxyphenyl)-2,2'-bipyridine (Br-Ph(6-{4-MeOPh})bpy) and 6-(2-bromophenyl)-3-(4-methoxyphenyl)-2,2'-bipyridine (Br-Ph(7-{4-MeOPh})bpy): Starting material: 0.96 g 4'-methoxyacetophenone. The crude product was purified by flash chromatography (EtOAc/c -hexane 1/3) to give Br-Ph(6-{4-MeOPh})bpy as a white solid (yield: 0.8 g, 1.9 mmol, 58%) and Br-Ph(7-{4-MeOPh})bpy as yellow oil (yield: 0.2 g, 0.5 mmol, 17%). Br-Ph(6-{4-MeOPh})bpy: ^1H NMR (300 MHz, CDCl_3) $\delta = 8.72$ (d, 1H, $^3J_{HH} = 4.8$ Hz), 8.65 (d, 1H, $^4J_{HH} = 1.6$ Hz), 8.57 (d, 1H, $^3J_{HH} = 8.8$ Hz), 7.87–7.76 (m, 4H), 7.72 (t, 1H, $^3J_{HH} = 7.6$ Hz), 7.50–7.41 (m, 1H), 7.37–7.28 (m, 2H), 7.03 (d, 2H, $^3J_{HH} = 8.8$ Hz), 3.88 (s, 3H) ppm. ^{13}C NMR (75 MHz, CDCl_3) $\delta = 160.73$, 158.26, 156.53, 156.42, 149.26, 148.99, 141.71, 137.12, 133.72, 131.94, 130.81, 129.87, 128.70, 127.69, 123.98, 122.30, 121.95, 117.28, 114.74, 55.63 ppm. Br-Ph(7-{4-MeOPh})bpy: ^1H NMR (300 MHz, CDCl_3) $\delta = 8.51$ (d, 1H, $^3J_{HH} = 4.8$ Hz), 7.89–7.79 (m, 1H), 7.75–7.59 (m, 4H), 7.57–7.50 (m, 1H), 7.41 (t, 1H, $^3J_{HH} = 7.5$ Hz), 7.24–7.06 (m, 3H), 6.80 (d, 2H, $^3J_{HH} = 8.8$ Hz), 3.81 (s, 3H) ppm.

6-(2-Bromophenyl)-4-(3-methoxyphenyl)-2,2'-bipyridine (Br-Ph(6-{3-MeOPh})bpy) and 6-(2-bromophenyl)-3-(3-methoxyphenyl)-2,2'-bipyridine (Br-Ph(7-{3-MeOPh})bpy): Starting material: 0.96 g 3'-methoxyacetophenone. The crude product was purified by flash chromatography (EtOAc/c -hexane 1/6) to give Br-Ph(6-{3-MeOPh})bpy as a white solid (yield: 0.7 g, 1.6 mmol, 49%) and Br-Ph(7-{3-MeOPh})bpy as yellow oil (yield: 0.5 g, 1.2 mmol, 37%). Br-Ph(6-{3-MeOPh})bpy: EI-MS: 418 [M⁺] m/z, calc. 418. ^1H NMR (300 MHz, CD_2Cl_2) $\delta = 8.76$ –8.67 (m, 2H), 8.53 (d, 1H, $^3J_{HH} = 8.0$ Hz), 7.89–7.80 (m, 2H), 7.80–7.67 (m, 2H), 7.54–7.39 (m, 3H), 7.39–7.29 (m, 3H), 7.03 (dt, 1H, $^3J_{HH} = 7.5$, $^4J_{HH} = 2.1$ Hz), 3.90 (s, 3H) ppm. ^{13}C NMR (75 MHz, CD_2Cl_2) $\delta = 160.29$, 158.10, 156.28, 155.97, 149.13, 149.10, 141.36, 139.83, 136.82, 133.39, 131.64, 130.11, 129.82, 127.56, 123.87, 122.60, 121.81, 121.30, 119.56, 117.49, 114.53, 112.76 ppm. Br-Ph(7-{3-MeOPh})bpy: ^1H NMR (300 MHz, CDCl_3) $\delta = 8.53$ (d, 1H, $^3J_{HH} = 4.8$ Hz), 7.88 (d, 1H, $^3J_{HH} = 8.0$ Hz), 7.78–7.72 (m, 1H), 7.72–7.59 (m, 3H), 7.57–7.50 (m, 1H), 7.45–7.37 (m, 1H), 7.30–7.13 (m, 3H), 6.85–6.77 (m, 2H),

6.73 (d, 1H, $^4J_{HH} = 1.8$ Hz), 3.66 (s, 3H) ppm. ^{13}C NMR (75 MHz, CDCl_3) δ = 159.31, 158.37, 156.75, 149.01, 140.53, 138.32, 136.20, 135.08, 133.39, 133.14, 131.79, 129.80, 129.25, 127.61, 124.96, 124.21, 122.56, 121.92, 121.81, 114.60, 113.33, 110.20, 55.30 ppm.

6-(2-Bromophenyl)-3-methyl-2,2'-bipyridine (Br-Ph(7-CH₃)bpy): Starting material: 0.37 g acetone. Yellow/orange oil. Yield: 1.0 g, 3.1 mmol, 98%. ^1H NMR (400 MHz, CDCl_3) δ = 8.67 (d, 1H, $^3J_{HH} = 4.7$ Hz), 7.93 (d, 1H, $^3J_{HH} = 7.9$ Hz), 7.80 (td, 1H, $^3J_{HH} = 7.7$, $^4J_{HH} = 1.7$ Hz), 7.68 (t, 2H, $^3J_{HH} = 8.0$ Hz), 7.58 (dd, 1H, $^3J_{HH} = 7.7$, $^4J_{HH} = 1.6$ Hz), 7.52 (d, 1H, $^3J_{HH} = 7.9$ Hz), 7.40–7.34 (m, 1H), 7.31–7.18 (m, 2H), 2.58 (s, 3H) ppm. ^{13}C NMR (101 MHz, CDCl_3) δ = 159.18, 155.81, 155.39, 148.38, 141.32, 139.46, 136.89, 133.50, 131.80, 131.45, 129.70, 127.69, 124.81, 124.04, 122.86, 122.21, 20.00 ppm.

6-(2-Bromophenyl)-3-trifluoromethyl-2,2'-bipyridine (Br-Ph(7-CF₃)bpy): Starting material: 0.72 g 1,1,1-trifluoroacetone. Yellowish solid after recrystallization. Yield: 1.2 g, 3.1 mmol, 98%. ^1H NMR (400 MHz, CDCl_3) δ = 8.70 (d, 1H, $^3J_{HH} = 4.8$ Hz), 8.18 (d, 1H, $^3J_{HH} = 8.3$ Hz), 7.85–7.75 (m, 2H), 7.70–7.66 (m, 1H), 7.59 (dd, 1H, $^3J_{HH} = 7.7$, $^4J_{HH} = 1.7$ Hz), 7.43–7.32 (m, 1H), 7.30–7.24 (m, 1H) ppm. ^{13}C NMR (101 MHz, CDCl_3) δ = 160.41, 157.10, 156.40, 148.97, 139.96, 136.70, 135.59, 133.67, 131.80, 130.61, 127.90, 124.19, 124.05, 123.91, 123.79, 123.74, 121.83 ppm. ^{19}F NMR (376 MHz, CDCl_3) δ = -57.44 ppm.

6-(2-Bromo-5-methoxyphenyl)-3-methyl-2,2'-bipyridine (Br-(MeO)Ph(7-CH₃)bpy): Starting material: 0.37 g acetone. Yellow oil. Yield: 1.1 g, 3.1 mmol, 97%. ^1H NMR (300 MHz, CDCl_3) δ = 8.69–8.68 (m, 1H), 7.95 (d, 1H, $^3J_{HH} = 7.7$ Hz), 7.88–7.75 (m, 1H), 7.75–7.63 (m, 1H), 7.63–7.47 (m, 1H), 7.37–7.23 (m, 1H), 7.15 (d, 1H, $^4J_{HH} = 3.0$ Hz), 6.90–6.73 (m, 1H), 3.79 (s, 3H), 2.58 (s, 3H) ppm.

6-(2-Bromo-5-methoxyphenyl)-3-trifluoromethyl-2,2'-bipyridine (Br-(MeO)Ph(7-CF₃)bpy): Starting material: 0.72 g 1,1,1-trifluoroacetone. Yellow solid. Yield: 1.3 g, 3.2 mmol, 99%. ^1H NMR (300 MHz, CDCl_3) δ = 8.78–8.68 (m, 1H), 8.21 (d, 1H, $^3J_{HH} = 8.5$ Hz), 7.90–7.84 (m, 1H), 7.84–7.82 (m, 1H), 7.82–7.79 (m, 1H), 7.58 (d, 1H, $^3J_{HH} = 8.9$ Hz), 7.43–7.35 (m, 1H), 7.15 (d, 1H, $^4J_{HH} = 3.0$ Hz), 6.88 (dd, 1H, $^3J_{HH} = 8.9$, $^4J_{HH} = 3.1$ Hz), 3.82 (s, 3H) ppm. ^{13}C NMR (75.5 MHz, CDCl_3) δ = 160.2, 159.1, 156.9, 156.3, 148.8, 140.5, 136.5, 135.4, 134.2, 125.4, 124.2, 124.0, 123.8, 123.6, 121.8, 116.8, 116.7, 112.0, 55.6 ppm. ^{19}F NMR (282.40 MHz, CDCl_3) δ = -57.51 ppm.

Synthesis of Ligands by Kröhnke Pyridine Synthesis - general procedure: A suspension of *N*-(1-(2-pyridinyl)-1-oxo-2-ethyl)pyridiniumiodide (5.22 g, 16.0 mmol, 1 eq.) and ammonium acetate (12.3 g, 160.0 mmol, 10 eq.) in 40 mL of glacial acetic acid was refluxed for 20 min. After addition of the corresponding Mannich reagent or chalkone (16.0 mmol, 1 eq.) the solution was refluxed for further 20 h. After cooling to ambient temperature the solvent was removed and the dark oil was diluted with 100 mL of chloroform and 100 mL of water. After mixing the layers the formed dark solid was filtered off and the organic layer was washed again with 100 mL of water and 100 mL of a saturated Na_2CO_3 solution. After removing the solvent the raw product was cleaned by filtration through silica (EtOAc/c-hexane 1/9). The products were received as bright brown to colorless solids.^[5]

6-(3-Methoxyphenyl)-2,2'-bipyridine (H-(MeO)Phbpy): Starting material: 3.90 g 1-(3-methoxyphenyl)-3-(dimethylamino)propan-1-one hydrochloride. Colorless solid. Yield: 1.2 g, 4.6 mmol, 29%. ^1H NMR (300 MHz, DMSO-d_6) δ = 8.71 (dt, 1H, $^3J_{HH} = 4.7$, $^4J_{HH} = 1.3$ Hz), 8.60–8.54 (m, 1H), 8.35 (dd, 1H, $^3J_{HH} = 5.8$, $^4J_{HH} = 2.9$ Hz), 8.07–7.95 (m, 3H), 7.83–7.75 (m, 2H), 7.51–7.41 (m, 2H), 7.05 (dd, 1H, $^3J_{HH} = 8.2$, $^4J_{HH} = 3.4$ Hz), 3.87 (s, 3H) ppm. ^{13}C NMR (75 MHz, DMSO-d_6) δ = 159.75, 155.24, 155.20, 154.90, 149.26, 139.91, 138.38, 137.40, 129.91, 124.28, 120.64, 119.23, 118.97, 114.77, 112.07, 55.19 ppm.

6-(2-Bromophenyl)-4-(2-methylphenyl)-2,2'-bipyridine (Br-Ph(6-{2-CH₃Ph}bpy): Starting material: 4.82 g 1-(2-bromophenyl)-3-(2-methylphenyl)-prop-2-en-1-on. White solid. Yield: 1.3 g, 3.4 mmol, 21%. ^1H NMR (300 MHz, CD_2Cl_2) δ = 8.58 (d, 1H, $^3J_{HH} = 4.4$ Hz), 8.46 (d, 1H, $^3J_{HH} = 8.0$ Hz), 8.36 (d, 1H, $^4J_{HH} = 1.5$ Hz), 7.76 (t, 1H, $^3J_{HH} = 7.8$ Hz), 7.65 (d, 1H, $^3J_{HH} = 8.0$ Hz), 7.62 (d, 1H, $^3J_{HH} = 7.7$ Hz), 7.52 (d, 1H, $^4J_{HH} = 1.5$ Hz), 7.39 (t, 1H, $^3J_{HH} = 7.5$ Hz), 7.25 (m, 6H), 2.32 (s, 3H) ppm. ^{13}C NMR (75 MHz, CD_2Cl_2) δ = 158.0, 156.6, 156.3, 151.3, 149.7, 142.0, 140.0, 137.4, 136.0, 133.9, 132.3, 131.2, 130.4, 130.0, 128.9, 128.1, 126.6, 125.7, 124.3, 121.8, 120.7, 20.8 ppm.

6-(2-Bromophenyl)-4-(3-nitrophenyl)-2,2'-bipyridine (Br-Ph(6-{3-NO₂Ph}bpy): Starting material: 5.31 g 1-(2-bromophenyl)-3-(3-nitrophenyl)-prop-2-en-1-on. Off white solid. Yield: 6.2 g, 14.4 mmol, 90%. ^1H NMR (300 MHz, CDCl_3) δ = 7.73 (d, 2H), 8.66 (m, 1H), 8.60–8.57 (m, 1H), 8.33 (dd, 1H), 8.16 (dd, 1H), 7.89–7.80 (m, 2H), 7.76–7.68 (m, 3H), 7.53–7.45 (m, 1H), 7.38–7.30 (m, 2H) ppm. ^{13}C NMR (75 MHz, CDCl_3) δ = 158.82, 157.03, 155.82, 149.37, 147.03, 141.06, 140.47, 137.26, 133.81, 133.46, 131.89, 130.36, 130.28, 127.89, 124.39, 123.97, 122.71, 122.42, 122.19, 121.96, 117.77 ppm.

Bromination of the methoxy-substituted derivatives – general procedure: Under inert conditions the ligand precursor (2.0 mmol, 1 eq.) was dissolved in 20 mL dry acetonitrile. Slowly, a solution of *N*-bromosuccinimide (0.39 g, 2.2 mmol, 1.1 eq.) in 10 mL dry acetonitrile was added and the reaction mixture was stirred at ambient temperature for 23 h. The product was precipitated by adding 150 mL of water and could be obtained pure by filtration.^[6]

6-(2-Bromo-5-methoxyphenyl)-2,2'-bipyridine (Br-(MeO)Phbpy): Starting material: 0.52 g 6-(3-methoxyphenyl)-2,2'-bipyridine. Colorless crystals. Yield: 0.5 g, 1.5 mmol, 75%. ^1H NMR (300 MHz, CD_2Cl_2) δ = 8.72–8.63 (m, 1H), 8.55–8.39 (m, 2H), 7.97–7.76 (m, 2H), 7.66–7.55 (m, 2H), 7.33 (ddd, 1H, $^3J_{HH} = 7.5$, $^4J_{HH} = 4.8$, $^5J_{HH} = 1.2$ Hz), 7.18 (d, 1H, $^4J_{HH} = 3.1$ Hz), 6.88 (dd, 1H, $^3J_{HH} = 8.8$, $^4J_{HH} = 3.1$ Hz), 3.84 (s, 3H) ppm. ^{13}C NMR (75 MHz, CD_2Cl_2) δ = 159.09, 157.42, 155.88, 155.52, 149.08, 142.17, 136.85, 136.80, 134.00, 124.44, 123.79, 121.11, 119.55, 116.95, 115.72, 112.01, 55.60 ppm.

5-(2-Bromo-5-methoxyphenyl)-3-(2-pyridinyl)-1,2,4-triazine (Br-(MeO)PhTriazPy): Starting material: 0.53 g 5-(3-methoxyphenyl)-3-(2-pyridinyl)-1,2,4-triazine. Yellow solid. Yield: 0.5 g, 1.5 mmol, 73%. ^1H NMR (300 MHz, CD_2Cl_2) δ = 9.65 (s, 1H), 8.91–8.82 (m, 1H), 8.62 (d, 1H, $^3J_{HH} = 7.9$ Hz), 7.96 (td, 1H, $^3J_{HH} = 7.8$, $^4J_{HH} = 1.8$ Hz), 7.66 (d, 1H, $^3J_{HH} = 8.8$ Hz), 7.57–7.46 (m, 1H), 7.29 (d, 1H, $^4J_{HH} = 3.1$ Hz), 7.01 (dd, 1H, $^3J_{HH} = 8.8$, $^4J_{HH} = 3.1$ Hz), 3.87 (s, 3H) ppm.

Synthesis of Biscycloocta-1,5-dienenickel(0) ($[\text{Ni}(\text{COD})_2]$): A three neck round bottom schlenk flask was loaded with 3.85 g (15 mmol, 1 eq.) nickel acetylacetone evacuated and heated with a heat gun. After cooling to ambient temperature 8 mL of cycloocta-1,5-diene and 20 mL of freshly distilled THF were added and the slush was cooled to -78°C using a dry ice/isopropyl alcohol bath. Through a dropping funnel 45 mL of a 1 M DIBAL-H (45 mmol, 3 eq) solution in *n*-hexane was added with a drop rate of 1.5 mL/min. After further 15 min the dark brown solution was warmed to 0°C and stirred for 1 h. The reaction mixture was stored over night at -18°C leading to the precipitation of a yellow solid. The black solution was disposed of and the resulting solid was dried under reduced pressure. Yield: 3.18 g, 11.6 mmol, 77%.^[7]

References:

- [1] Hage, R.; Prins, R.; Haasnoot, J.G.; Reedijk, J.; Vos, J.G., *J. Chem. Soc., Dalton Trans.* **1987**, 1389–1395.
- [2] Riley, H.L.; Morley, J.F.; Friend, N.A.C., *J. Chem. Soc.* **1932**, 0, 1875.
- [3] Pabst, G.R.; Sauer, J., *Tetrahedron Lett.* **1998**, 39, 6687–6690.
- [4] Wang, S.W.; Guo, W.S.; Wen, L.R.; Li, M., *RSC Adv.* **2014**, 4, 59218–59220.
- [5] Kröhnke, F., *Synthesis* **1976**, 1–24.
- [6] Zysman-Colman, E.; Arias, K.; Siegel, J.S., *Can. J. Chem.* **2009**, 87, 440–447.
- [7] Krysan, D.J.; Mackenzie, P.B., *J. Org. Chem.* **1990**, 55, 4229–4230.
- [8] Klein, A.; Rausch, B.; Kaiser, A.; Vogt, N.; Krest, A., *J. Organomet. Chem.* **2014**, 774, 86–93.

B Supporting Figures:

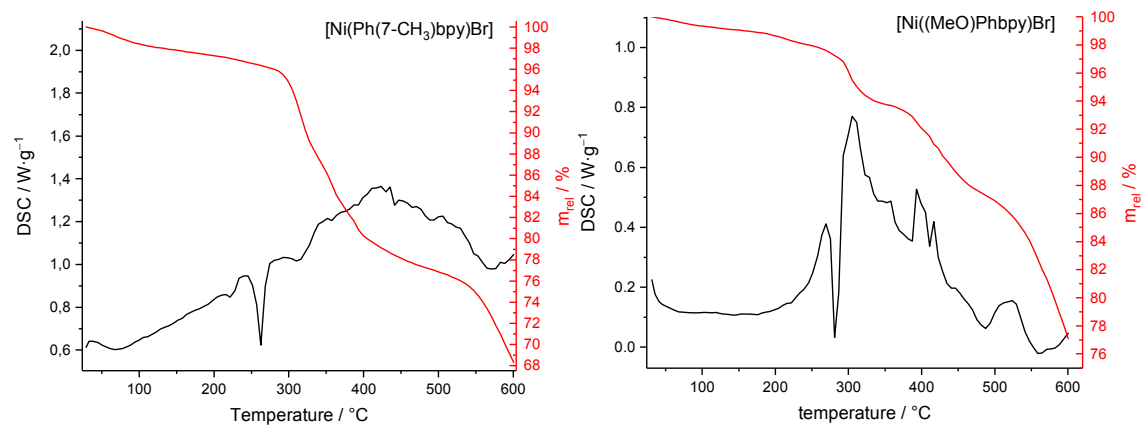


Figure S1. TG-DTA measurements of $[Ni(Ph(7-CH_3)bpy)Br]$ (left) and $[Ni((MeO)Phbpy)Br]$ (right).

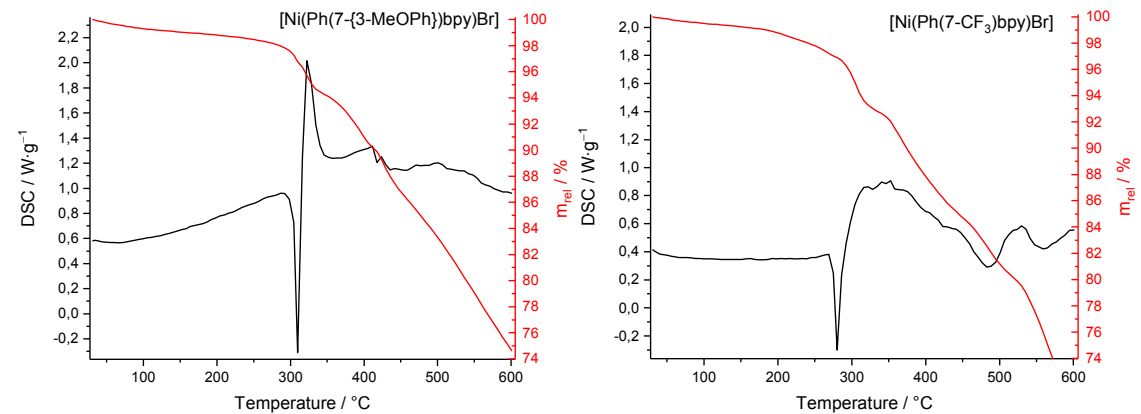


Figure S2. TG-DTA measurements of $[Ni(Ph(7-\{3-MeOPh\})bpy)Br]$ (left) and $[Ni(Ph(7-CF_3)bpy)Br]$ (right).

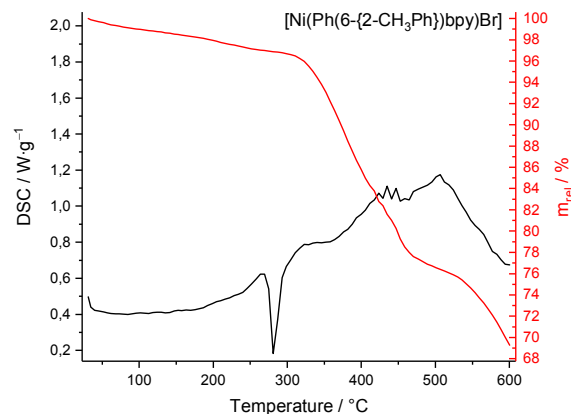


Figure S3. TG-DTA measurement of $[Ni(Ph(6-\{2-CH_3Ph\})bpy)Br]$.

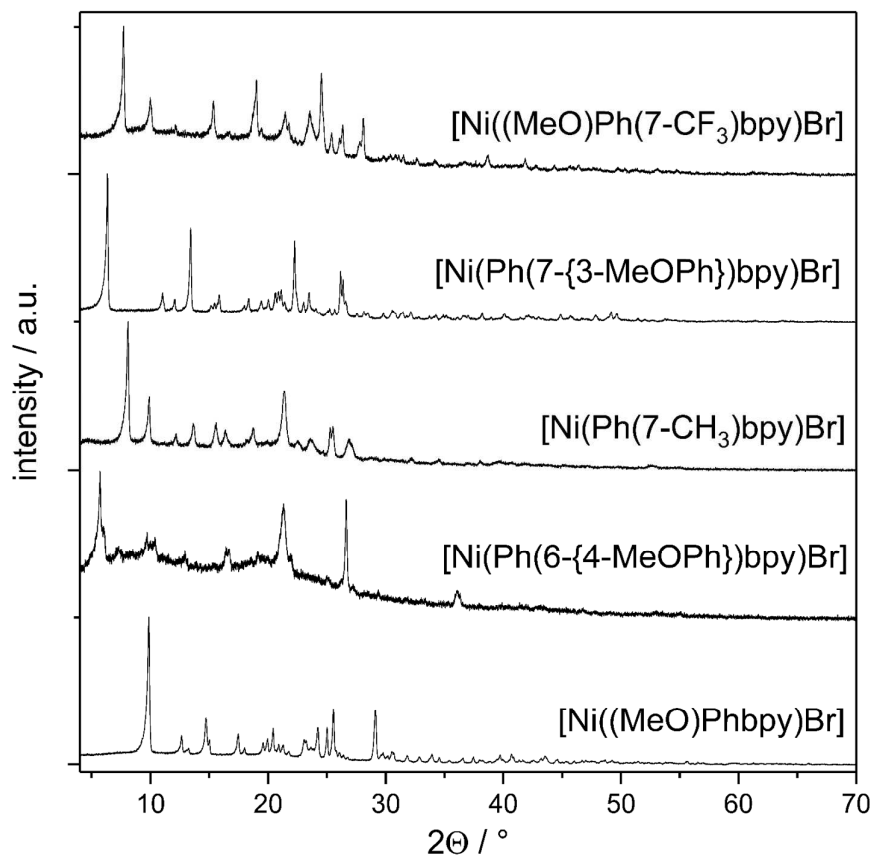


Figure S4. Powder XRD of (from top to bottom) $[\text{Ni}((\text{MeO})\text{Ph}(7\text{-CF}_3)\text{bpy})\text{Br}]$, $[\text{Ni}(\text{Ph}(7\text{-}\{3\text{-MeOPh}\})\text{bpy})\text{Br}]$, $[\text{Ni}(\text{Ph}(7\text{-CH}_3)\text{bpy})\text{Br}]$, $[\text{Ni}(\text{Ph}(6\text{-}\{4\text{-MeOPh}\})\text{bpy})\text{Br}]$, and $[\text{Ni}((\text{MeO})\text{Phbpy})\text{Br}]$ at ambient temperature.

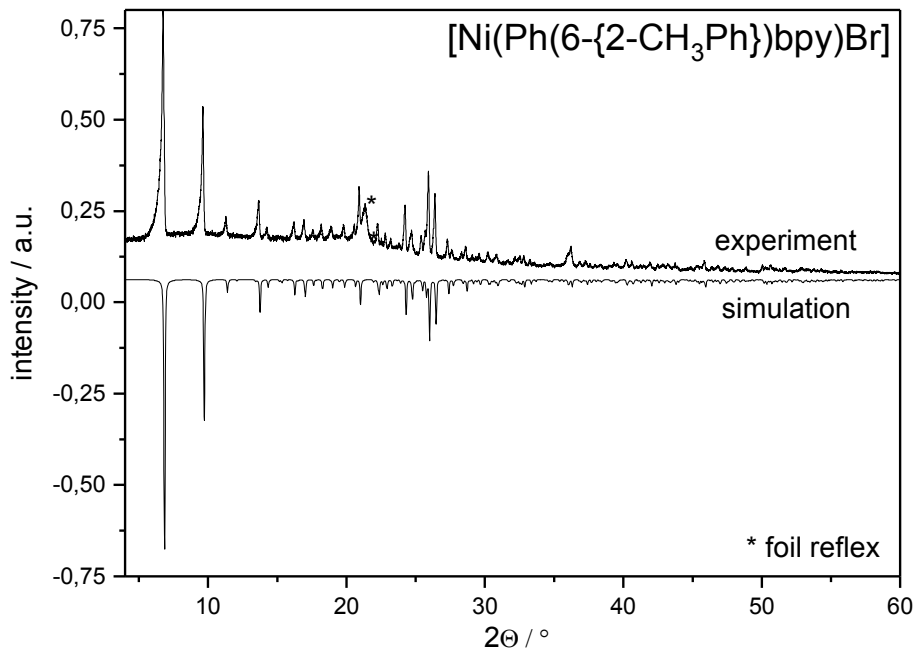


Figure S5. Powder XRD of $[\text{Ni}(\text{Ph}(6\text{-}\{2\text{-CH}_3\text{Ph}\})\text{bpy})\text{Br}]$ (upper trace) together with simulated data from single crystal data (lower trace) at ambient temperature.

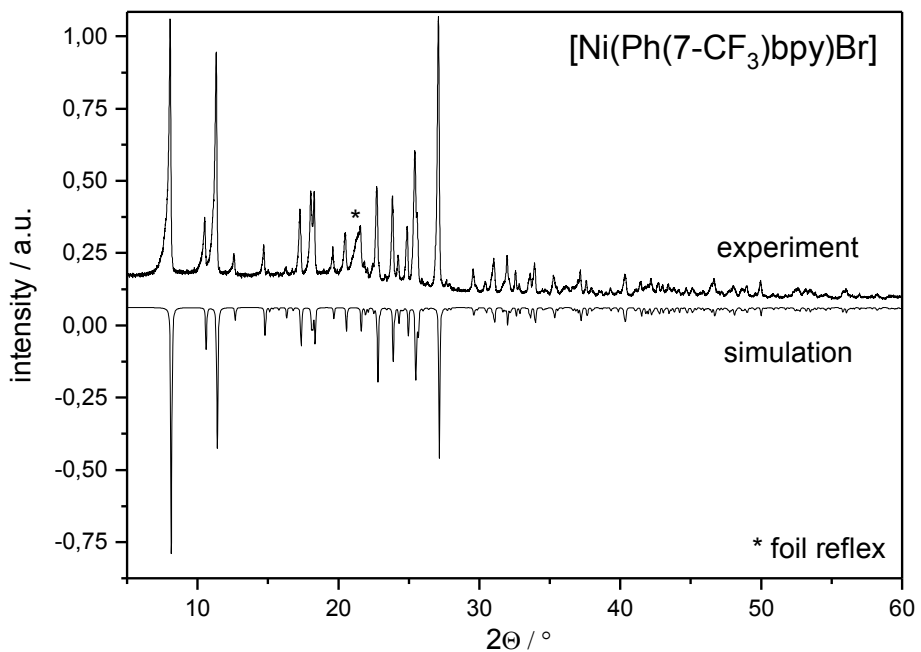


Figure S6. Powder XRD of $[\text{Ni}(\text{Ph}(7\text{-CF}_3)\text{bpy})\text{Br}]$ (upper trace) together with simulated data from single crystal data (lower trace) at ambient temperature.

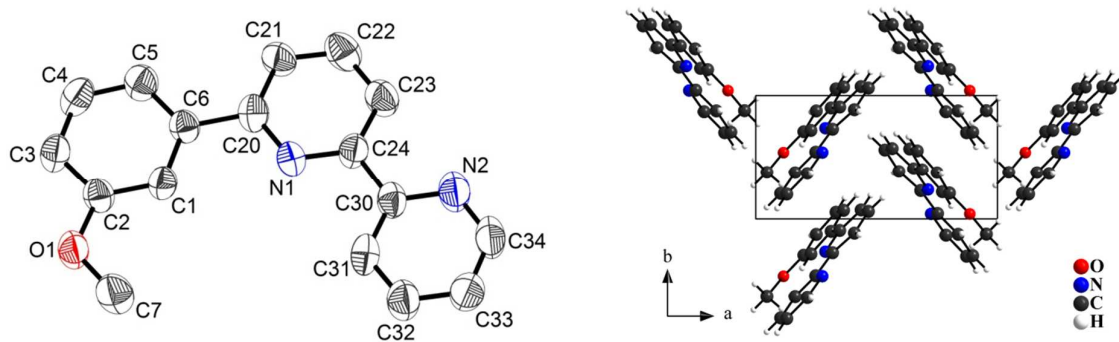


Figure S7. Molecular structure (left, H-atoms are omitted, ellipsoids at 50% probability) and crystal structure of H-(MeO)Phbpy (right, along the crystallographic c -axis).

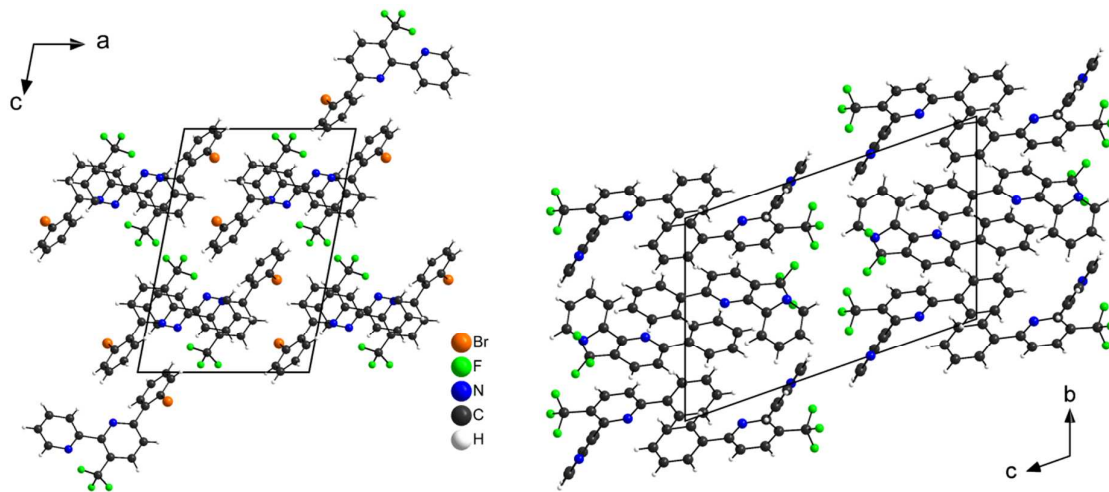


Figure S8. Crystal structures of $\text{Br}-\text{Ph}(7-\text{CF}_3)\text{bpy}$ (left, along crystallographic b -axis) and $\text{H}-\text{Ph}(7-\text{CF}_3)\text{bpy}$ (right, along the crystallographic a -axis).

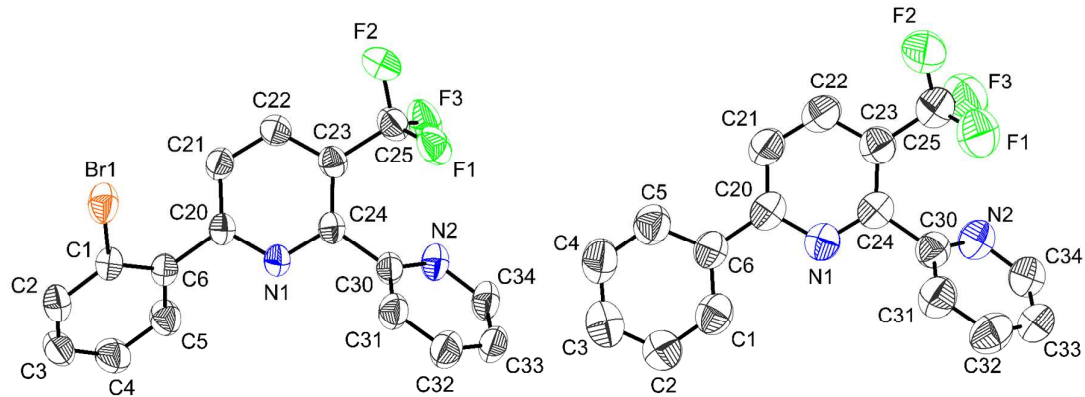


Figure S9. Molecular structures of $\text{Br}-\text{Ph}(7-\text{CF}_3)\text{bpy}$ (left) and $\text{H}-\text{Ph}(7-\text{CF}_3)\text{bpy}$ (right). H-atoms are omitted, ellipsoids at 50% probability.

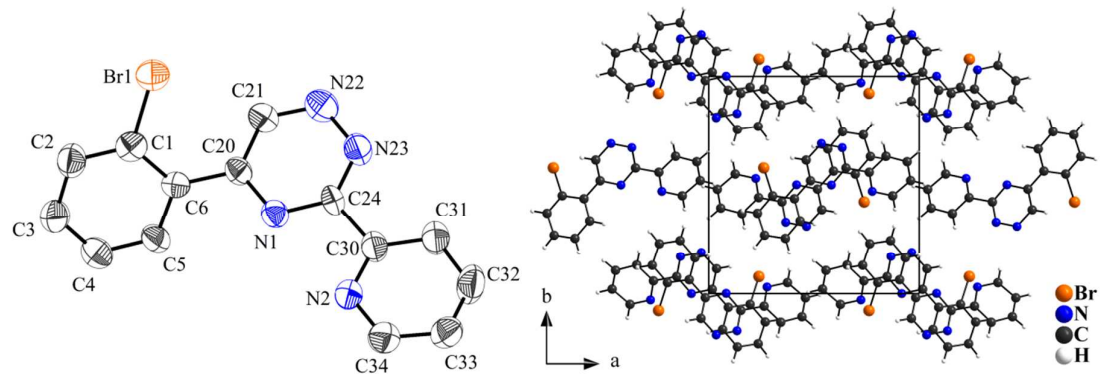


Figure S10. Molecular structure (left, H-atoms are omitted, ellipsoids at 50% probability) and crystal structure of $\text{Br}-\text{PhTriazPy}$ (right, along the crystallographic c -axis).

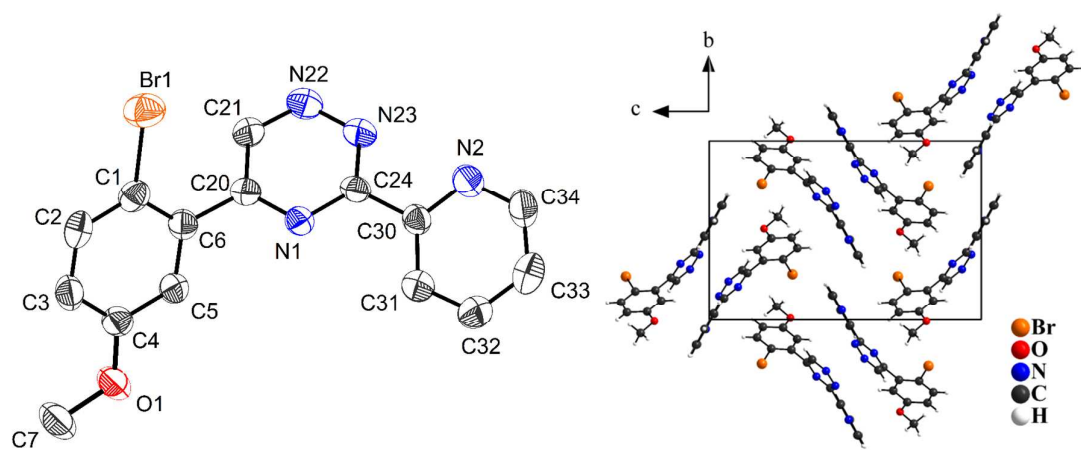


Figure S11. Molecular structure (left, H-atoms are omitted, ellipsoids at 50% probability) and crystal structure of $\text{Br}-(\text{MeO})\text{Ph}\text{TriazPy}$ (right, along the crystallographic a -axis).

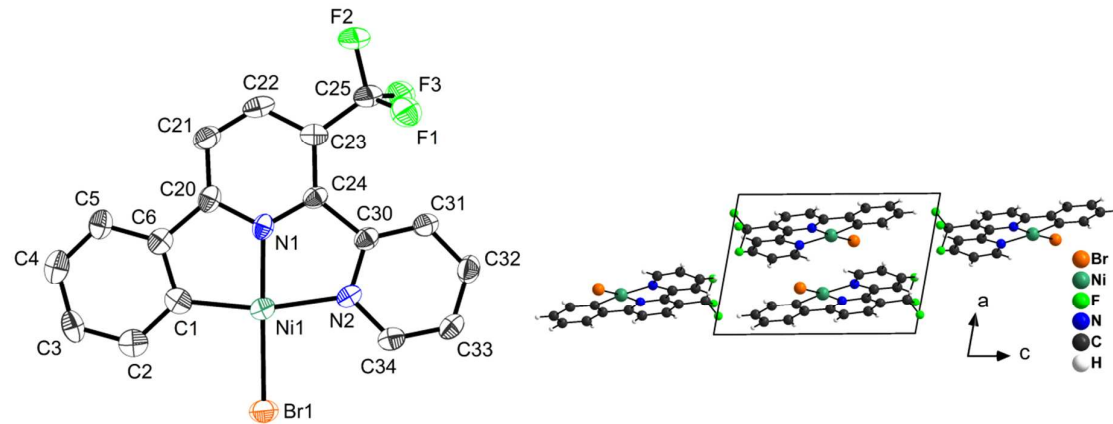


Figure S12. Molecular structure (left, H-atoms are omitted, ellipsoids at 50% probability) and crystal structure of $[\text{Ni}(\text{Ph}(7-\text{CF}_3)\text{bpy})\text{Br}]$ (right, along the crystallographic b -axis).

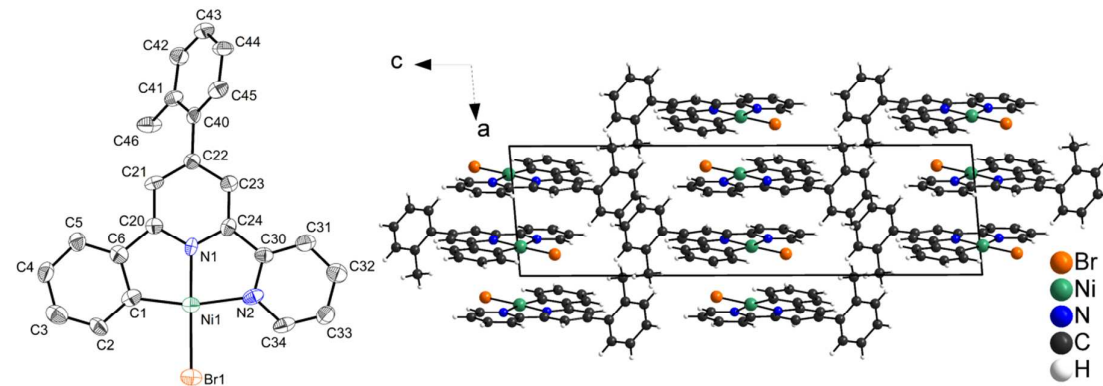


Figure S13. Molecular structure (left, H-atoms are omitted, ellipsoids at 50% probability) and crystal structure of $[\text{Ni}(\text{Ph}(6-\{2-\text{CH}_3\text{Ph}\})\text{bpy})\text{Br}]$ (right, along the crystallographic b -axis).

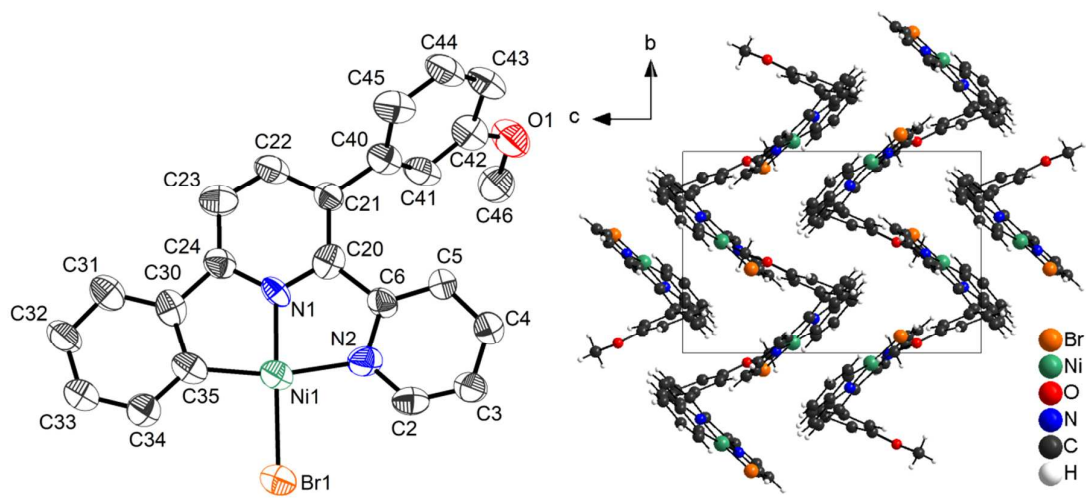


Figure S14. Molecular structure (left, H-atoms are omitted, ellipsoids at 50% probability) and crystal structure of $[\text{Ni}(\text{Ph}(7\text{-}\{3\text{-MeOPh}\})\text{bpy})\text{Br}]$ (right, along the crystallographic *a*-axis).

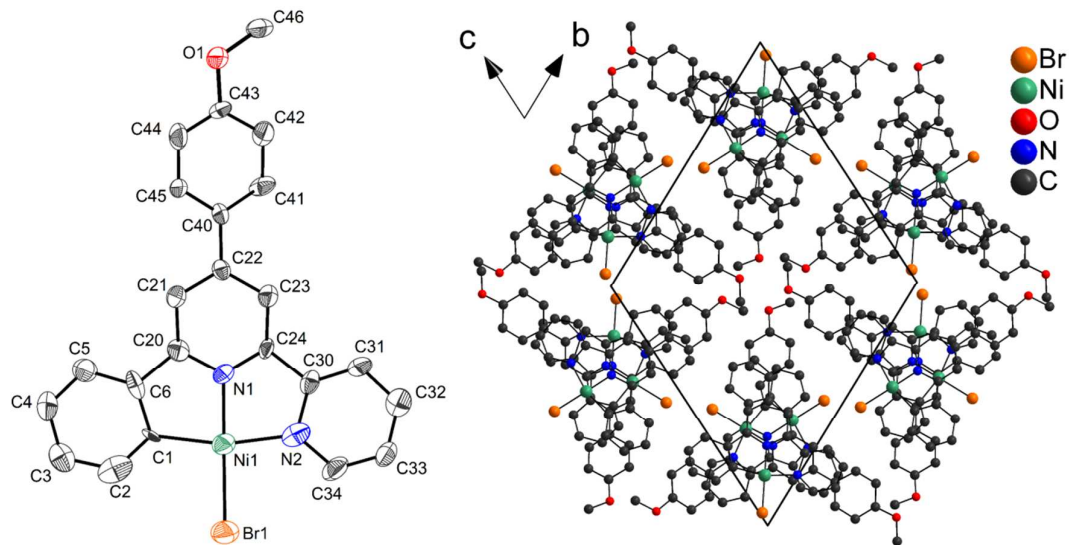


Figure S15. Molecular structure (left, H-atoms are omitted, ellipsoids at 50% probability) and crystal structure of $[\text{Ni}(\text{Ph}(6\text{-}\{4\text{-MeOPh}\})\text{bpy})\text{Br}]$ (right, along the crystallographic *a*-axis, H-atoms are omitted for clarity).

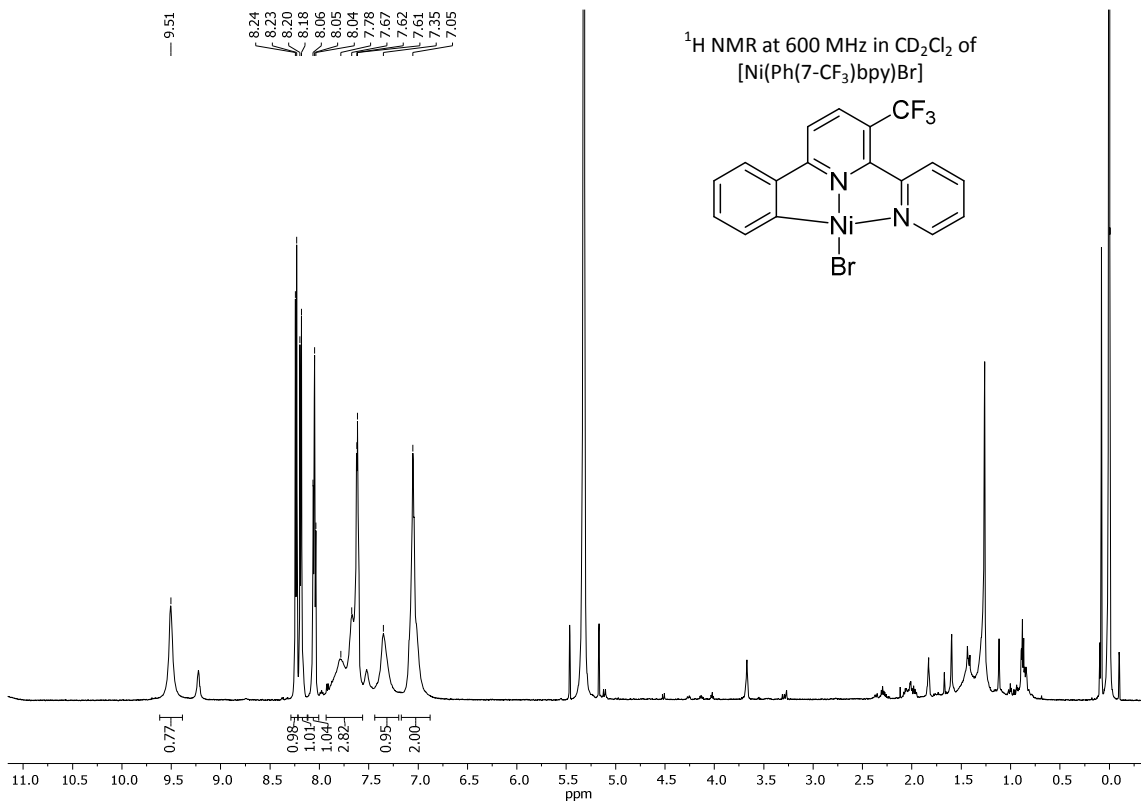


Figure S16. ¹H NMR spectrum of [Ni(Ph(7-CF₃)bpy)Br] in CD_2Cl_2 at 600 MHz.

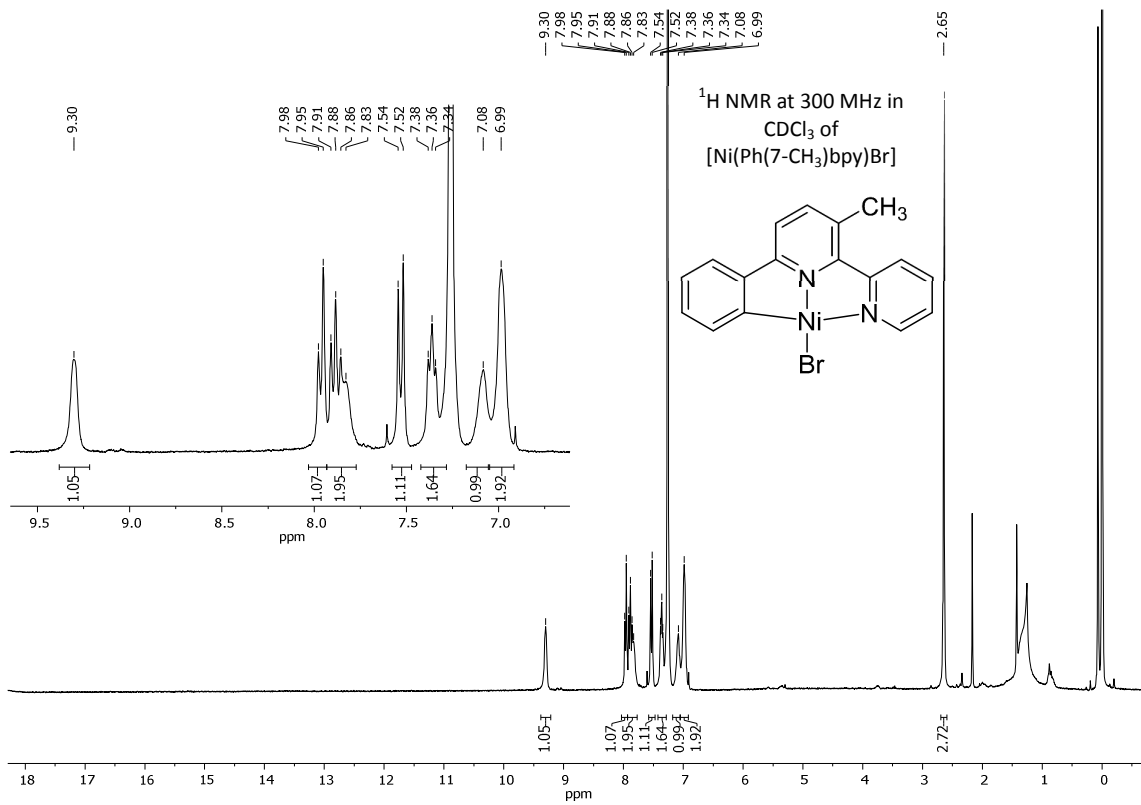


Figure S17. ¹H NMR spectrum of [Ni(Ph(7-CH₃)bpy)Br] in CDCl_3 at 300 MHz.

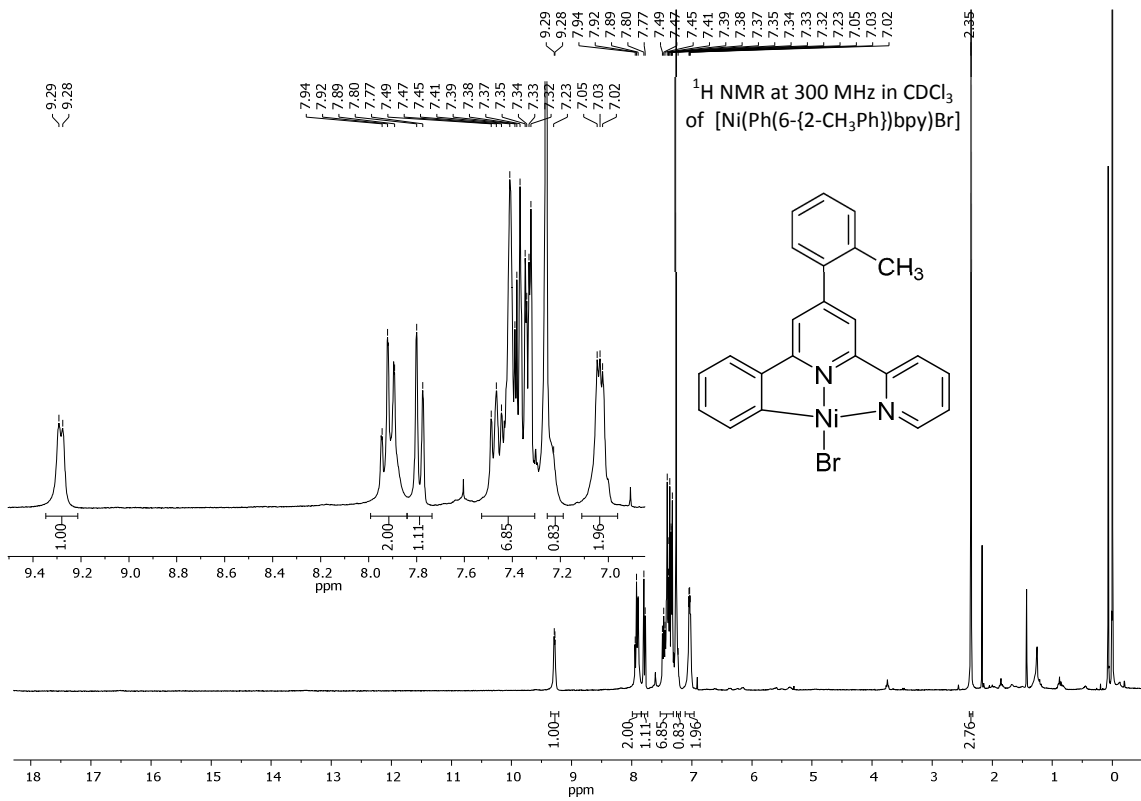


Figure S18. ¹H NMR spectrum of [Ni(Ph(6-{2-CH₃Ph})bpy)Br] in CDCl₃ at 300 MHz.

— [Ni((MeO)Phbpy)Br]	— [Ni(Ph(6-{2-CH ₃ Ph})bpy)Br]	— [Ni(Ph(6-{3-NO ₂ Ph})bpy)Br]
— [Ni(Ph(6-{3-MeOPh})bpy)Br]	— [Ni(Ph(6-{4-MeOPh})bpy)Br]	— [Ni(Ph(7-CH ₃)bpy)Br]
— [Ni(Ph(7-CF ₃)bpy)Br]	— [Ni(Ph(7-{3-MeOPh})bpy)Br]	— [Ni(Ph(7-{4-MeOPh})bpy)Br]
— [Ni(Ph(dc)bpy)Br]	— [Ni((MeO)Ph(7-CH ₃)bpy)Br]	— [Ni((MeO)Ph(7-CF ₃)bpy)Br]

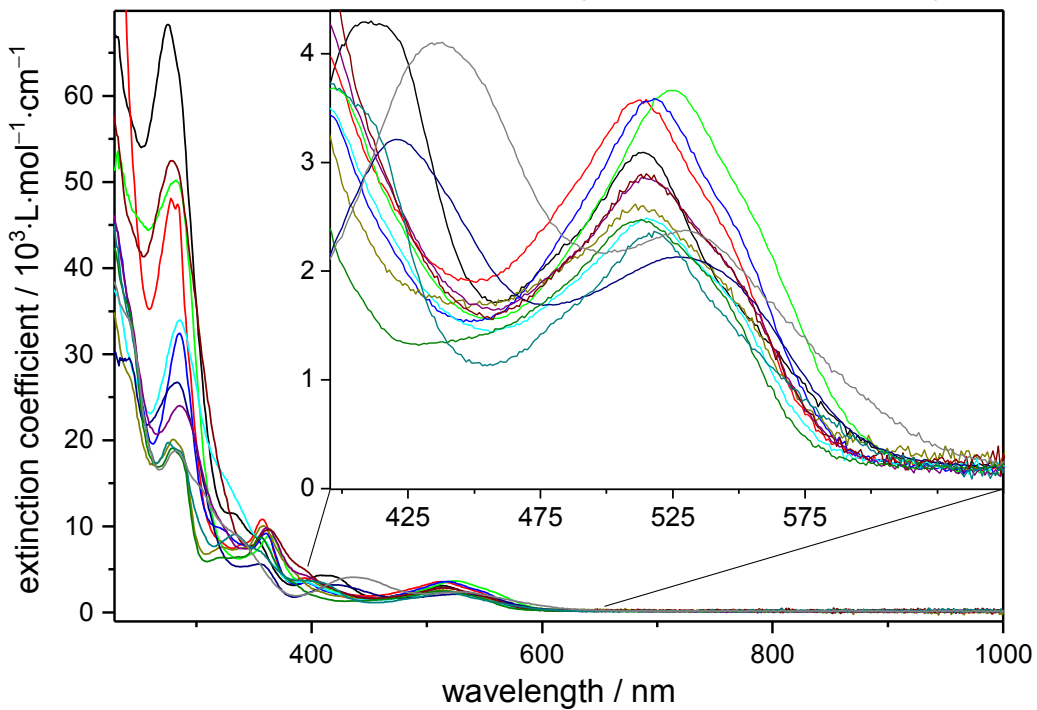


Figure S19. Absorption spectra of the complexes [Ni((R)Ph(R')bpy)Br] in THF at ambient temperature.

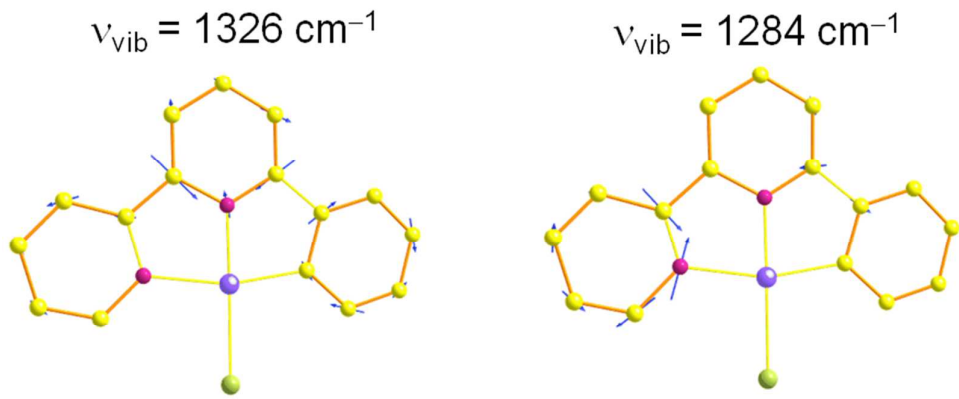


Figure S20. Selected DFT calculated skeletal vibrational modes of $[\text{Ni}(\text{Phbpy})\text{Br}]^{2-}$; arrows denote the scaled displacement vectors.

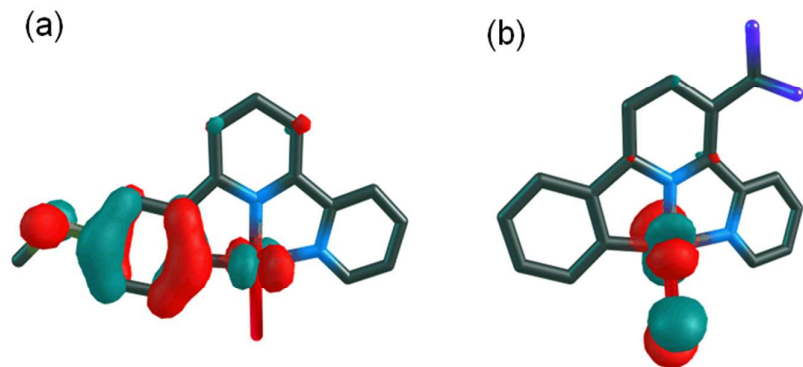


Figure S21. DFT calculated composition of the singly occupied molecular orbital (SOMO) of $[\text{Ni}((\text{MeO})\text{Phbpy})\text{Br}]^{2+}$ (a) and $[\text{Ni}(\text{Ph}(7\text{-CF}_3)\text{bpy})\text{Br}]^{2+}$ (b).

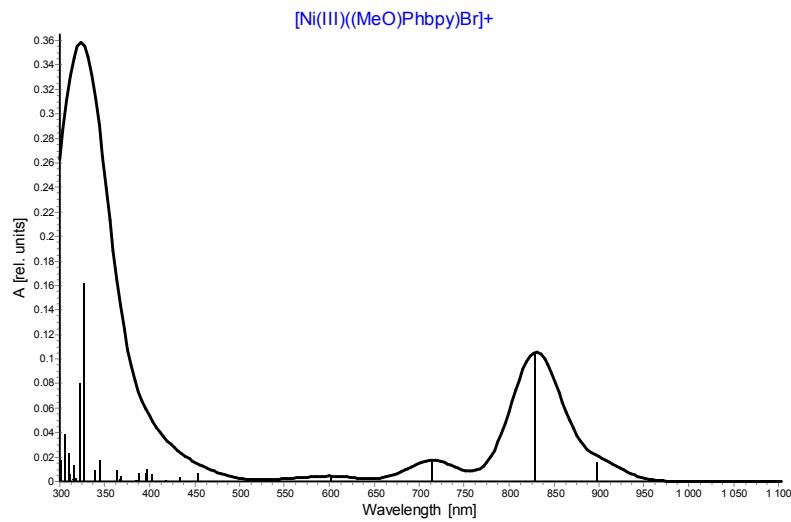


Figure S22. DFT calculated UV-vis absorptions of $[\text{Ni}(\text{III})(\text{(MeO})\text{Phbpy})\text{Br}]^{2+}$.

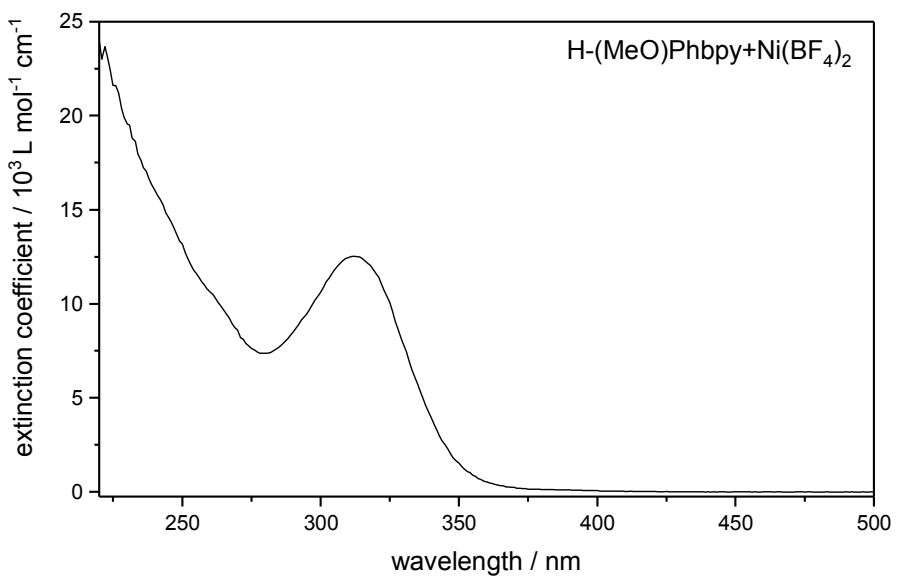


Figure S23. Absorption spectrum recorded after the reaction of $\text{Ni}(\text{BF}_4)_2$ with $\text{H}-(\text{MeO})\text{Phbpy}$ in THF at ambient temperature.

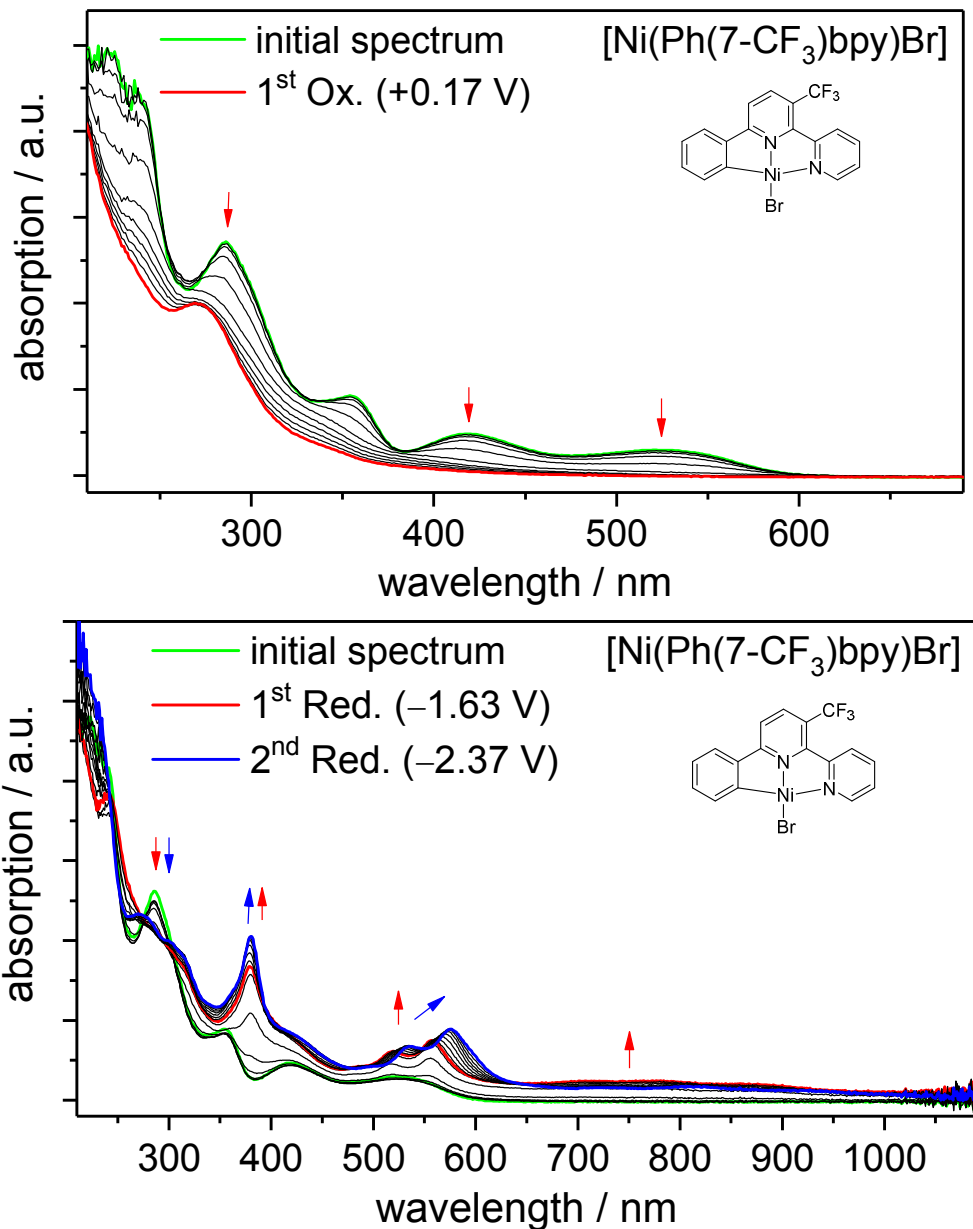


Figure S24. UV-vis spectra of $[\text{Ni}(\text{Ph}(7-\text{CF}_3)\text{bpy})\text{Br}]$ during electrochemical oxidation (upper) and reduction (lower), measured in 0.1 M $n\text{Bu}_4\text{NPF}_6$ /THF solution at rt. Potentials referenced vs. ferrocene/ferrocenium.

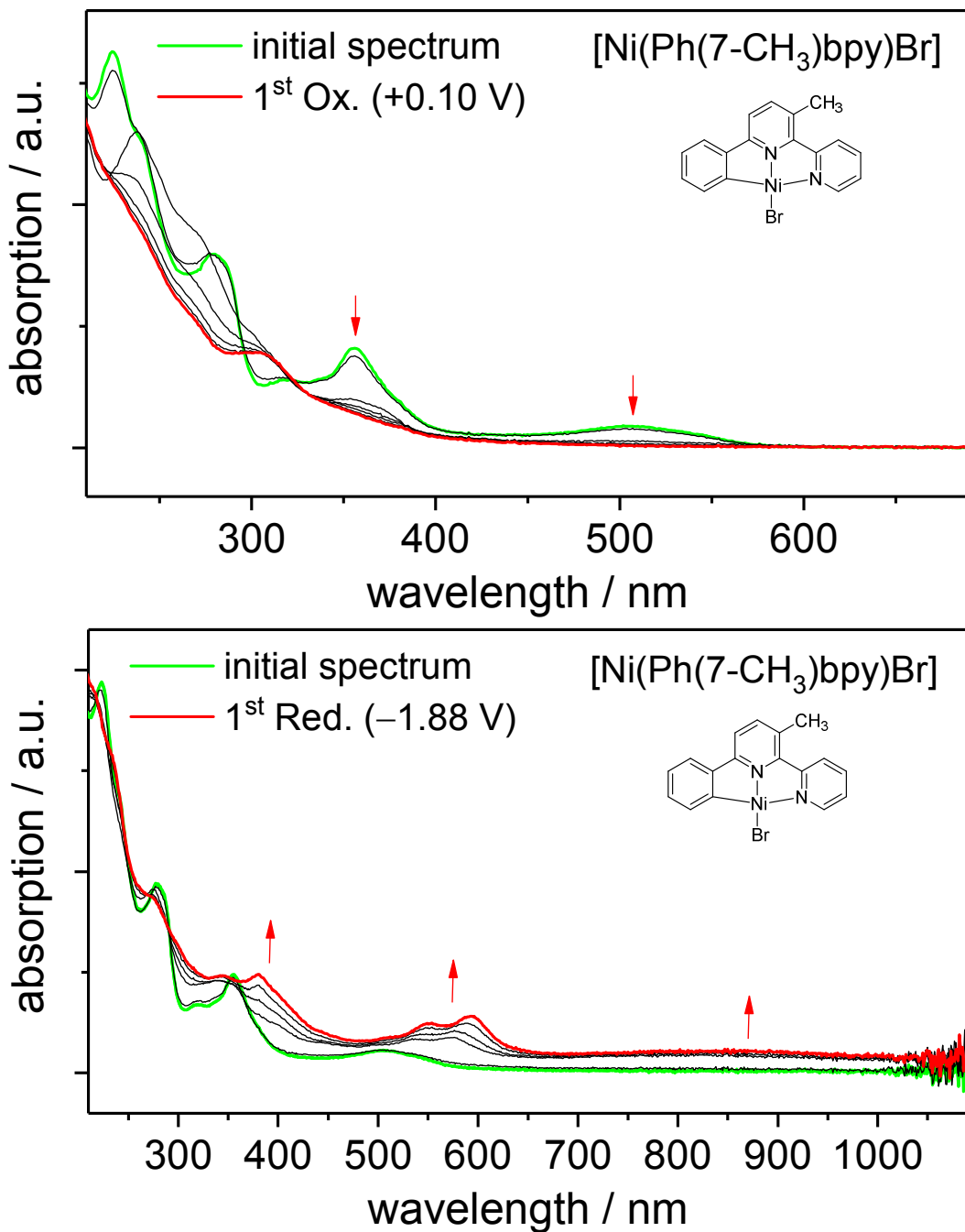


Figure S25. UV-vis spectra of $[\text{Ni}(\text{Ph}(7\text{-CH}_3)\text{bpy})\text{Br}]$ during electrochemical oxidation (upper) and reduction (lower), measured in 0.1 M $n\text{Bu}_4\text{NPf}_6$ /THF solution at rt. Potentials referenced vs. ferrocene/ferrocenium

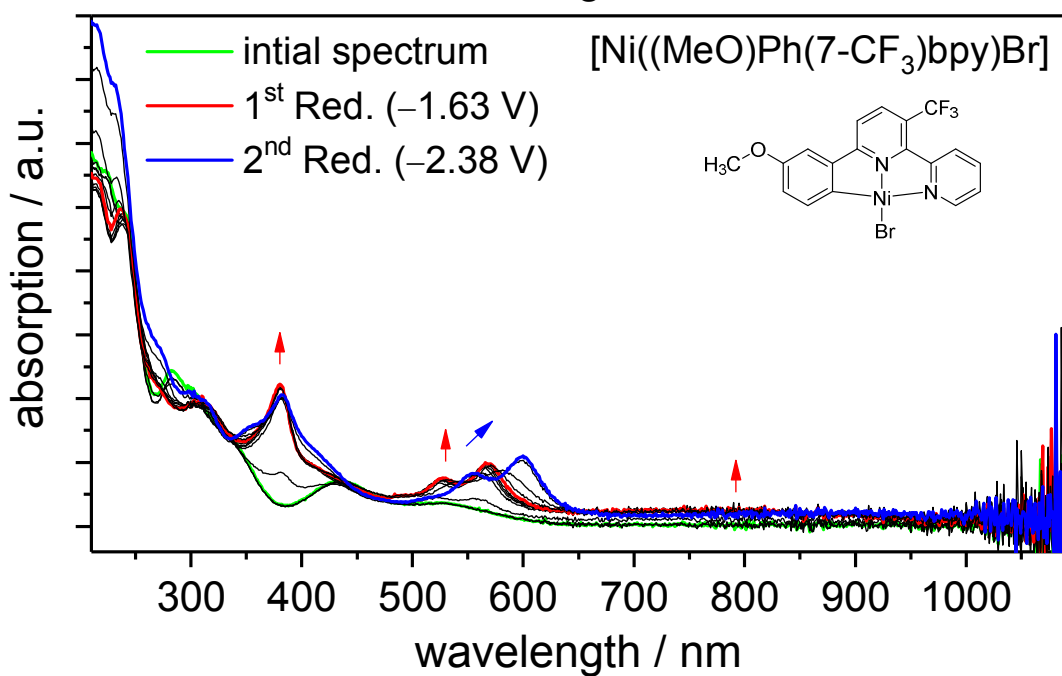
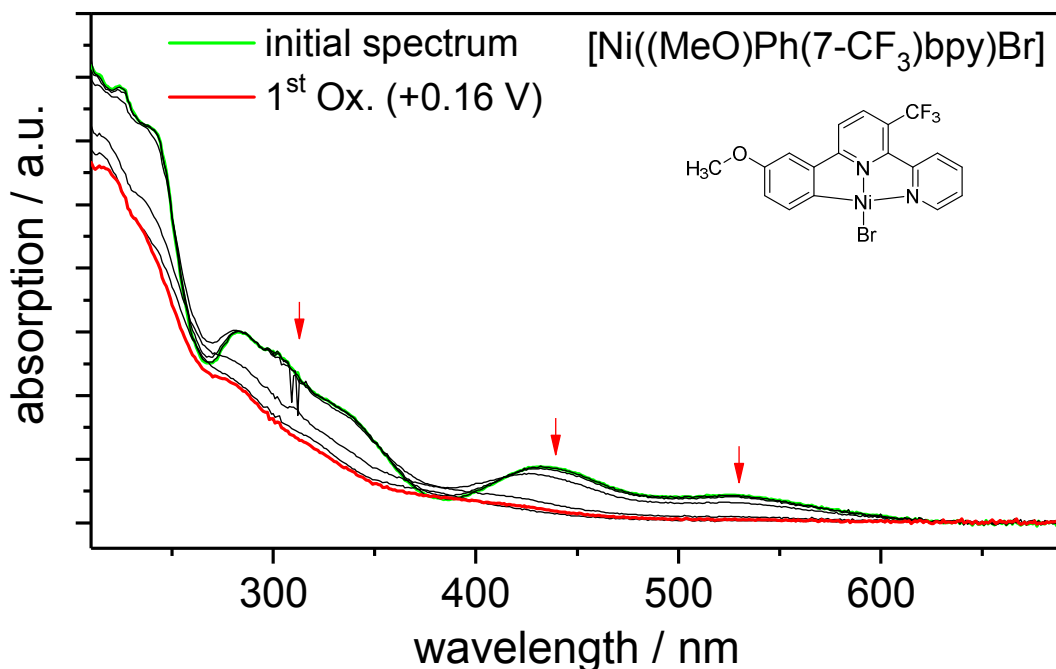


Figure S26. UV-vis spectra of [Ni((MeO)Ph(7-CF₃)bpy)Br] during electrochemical oxidation (upper) and reduction (lower), measured in 0.1 M *n*Bu₄NPF₆/THF solution at rt. Potentials referenced vs. ferrocene/ferrocenium

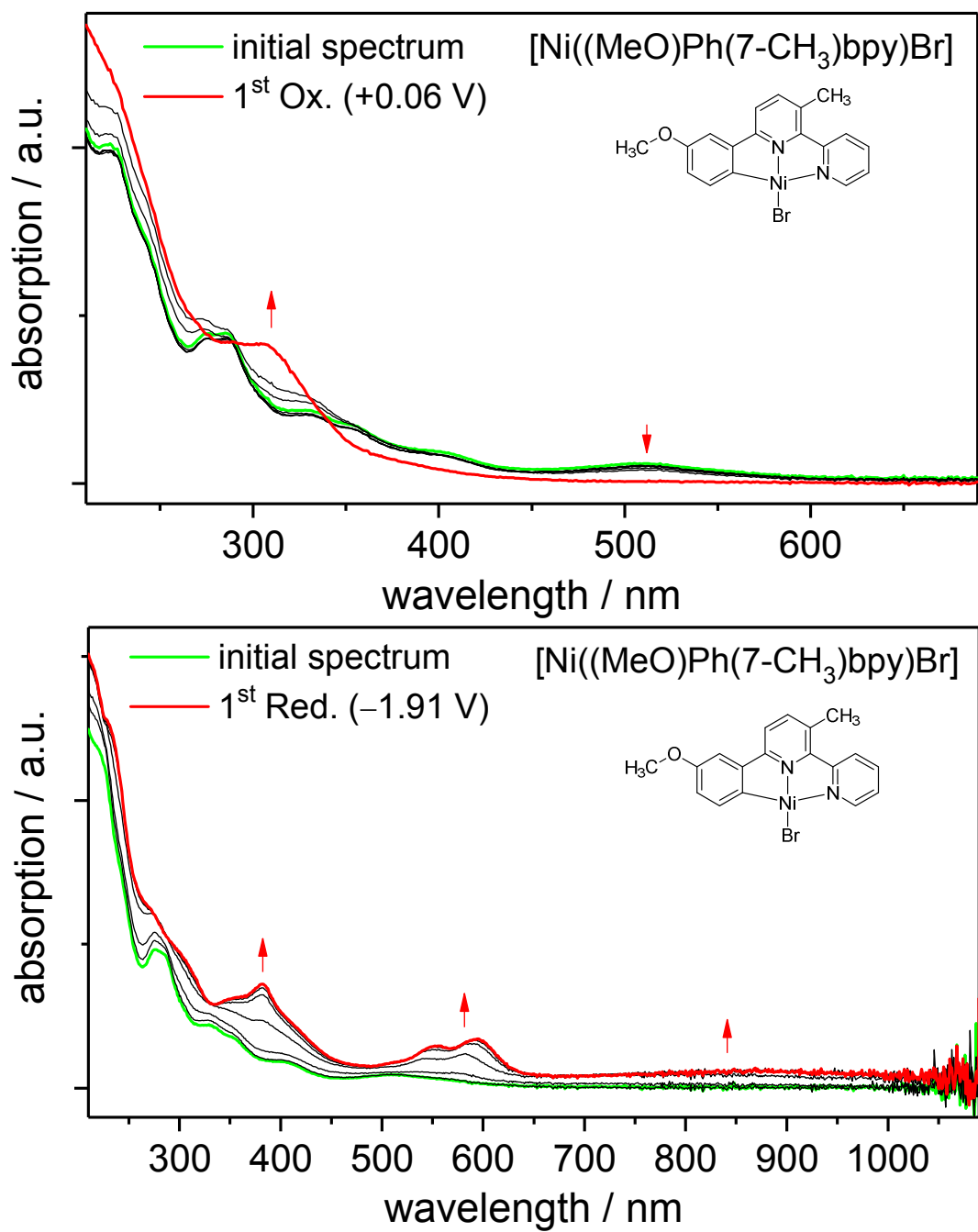


Figure S27. UV-vis spectra of $[\text{Ni}((\text{MeO})\text{Ph}(7-\text{CH}_3)\text{bpy})\text{Br}]$ during electrochemical oxidation (upper) and reduction (lower), measured in 0.1 M $n\text{Bu}_4\text{NPF}_6$ /THF solution at rt. Potentials referenced vs. ferrocene/ferrocenium

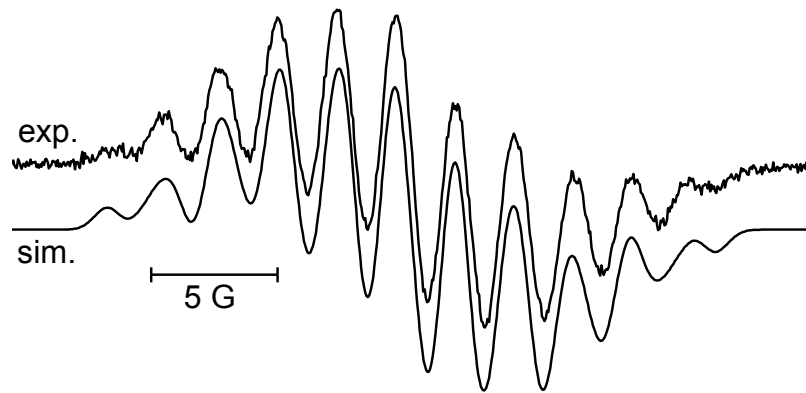


Figure S28. X Band EPR spectrum during electrochemical reduction of H-Phbpy in 0.1 M $n\text{Bu}_4\text{NPF}_6$ /THF solution at ambient temperature (upper) with simulation (lower). Simulation: $g_{\text{iso}} = 2.0029$. 2x $a_{\text{H}} = 4.40$ G, 2x $a_{\text{H}} = 1.75$ G, 1x $a_{\text{H}} = 0.90$ G, 2x $a_{\text{N}} = 2.49$ G. Measured with 9.473295 GHz.

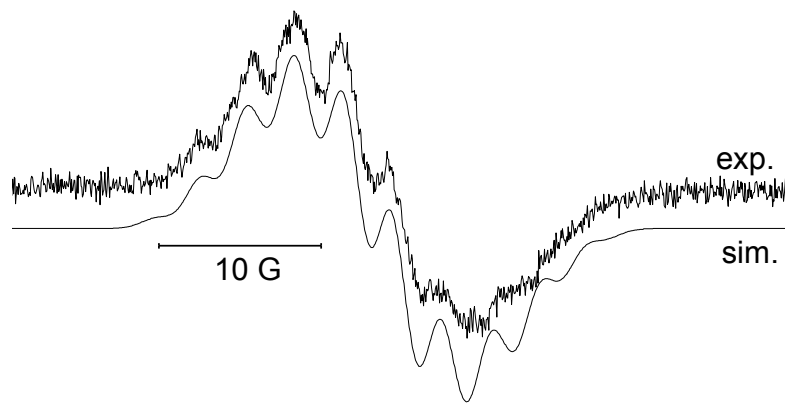


Figure S29. X Band EPR spectrum during electrochemical reduction of $[\text{Ni}(\text{Ph}(6-\{\text{2-CH}_3\text{Ph}\})\text{bpy})\text{Br}]$ in 0.1 M $n\text{Bu}_4\text{NPF}_6$ /THF solution at ambient temperature (upper) with simulation (lower). Simulation: $g_{\text{iso}} = 2.0021$ with 2x $a_{\text{H}} = 3.75$ G, 2x $a_{\text{H}} = 2.35$ G, $a_{\text{N}} = 2.75$ G. Measured with 9.471071 GHz.

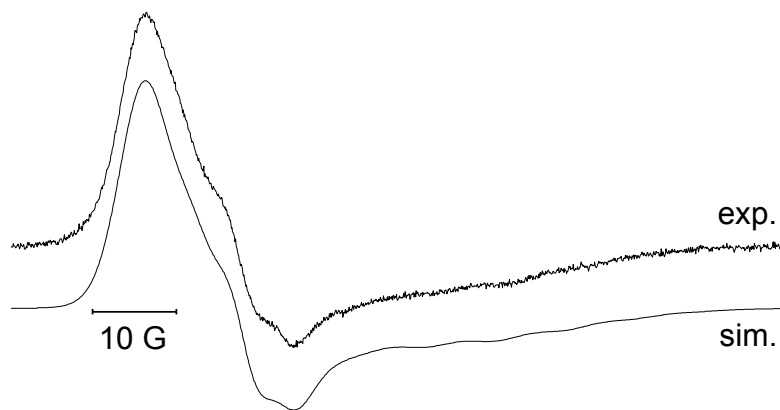


Figure S30. X Band EPR spectrum during electrochemical reduction of $[\text{Ni}(\text{Ph}(6-\{\text{2-CH}_3\text{Ph}\})\text{bpy})\text{Br}]$ in glassy frozen 0.1 M $n\text{Bu}_4\text{NPF}_6$ /THF solution at 110 K (upper) with simulation (lower). Simulation: $g_1 = 2.0125$, $g_2 = 2.0055$ with 2x $a_{\text{H}} = 4.6$ G, $g_3 = 1.988$ with 2x $a_{\text{H}} = 8.0$ G, 2x $a_{\text{N}} = 8.0$ G. Measured at 9.471071 GHz.

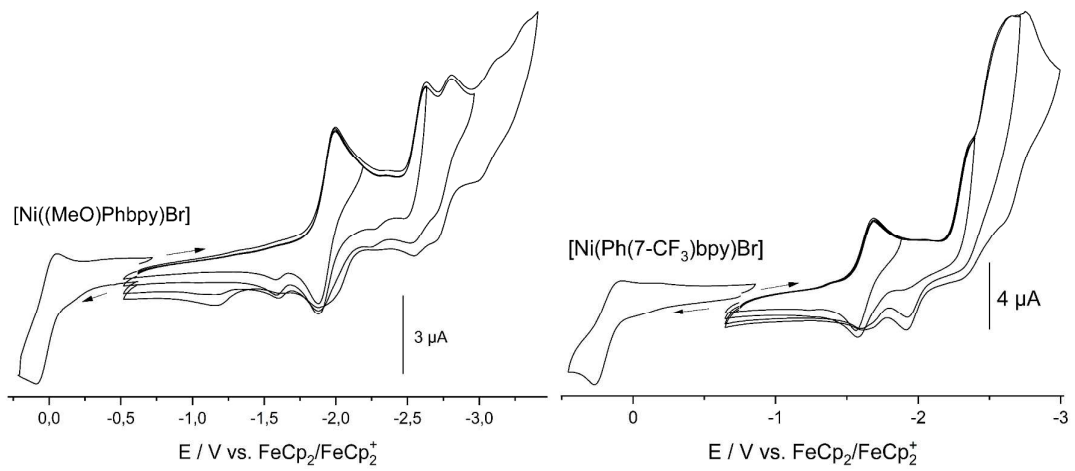


Figure S31. Cyclic voltammograms of $[\text{Ni}(\text{MeO})\text{Phbpy}\text{Br}]$ (left) and $[\text{Ni}(\text{Ph}(7-\text{CF}_3)\text{bpy})\text{Br}]$ (right) measured in $0,1 \text{ M } n\text{Bu}_4\text{NPF}_6/\text{THF}$ solution with a scan rate of 100 mV s^{-1} .

C Supporting Tables:

Table S1. Electrochemical data for the complexes $[\text{Ni}((\text{R})\text{Ph}(\text{R}')\text{bpy})\text{Br}]$.^a

$[\text{Ni}((\text{R})\text{Ph}(\text{R}')\text{bpy})\text{Br}]$	Ox. II	Ox. I	Red. A	Red. I	Red. II	Red. III	Red. IV
Phbpy ^b		0.10 $E_{1/2}$		-1.90 $E_{1/2}$	-2.58 E_{pc}	-2.70 E_{pc}	
(MeO)Phbpy		0.02 $E_{1/2}$		-1.94 $E_{1/2}$	-2.63 E_{pc}	-2.81 E_{pc}	
Ph(6-{2-CH ₃ Ph})bpy		0.11 $E_{1/2}$		-1.84 $E_{1/2}$	-2.47 $E_{1/2}$		
Ph(6-{3-NO ₂ Ph})bpy		0.13 E_{pa}	-1.63 $E_{1/2}$	-2.00 $E_{1/2}$	-2.54 E_{pc}	-2.66 E_{pc}	
Ph(6-{4-MeOPh})bpy	0.59 E_{pa}	0.14 E_{pa}		-1.84 $E_{1/2}$	-2.49 E_{pc}	-2.66 E_{pc}	
Ph(6-{3-MeOPh})bpy		0.09 $E_{1/2}$		-1.83 $E_{1/2}$	-2.42 $E_{1/2}$		
Ph(7-{4-MeOPh})bpy		0.09 $E_{1/2}$		-1.89 $E_{1/2}$	-2.53 $E_{1/2}$	-2.69 $E_{1/2}$	
Ph(7-{3-MeOPh})bpy		0.07 $E_{1/2}$		-1.83 $E_{1/2}$	-2.51 E_{pc}	-2.66 E_{pc}	-3.06 E_{pc}
Ph(7-CH ₃)bpy		0.10 $E_{1/2}$		-1.88 $E_{1/2}$	-2.58 E_{pc}	-2.72 E_{pc}	-3.09 E_{pc}
Ph(7-CF ₃)bpy		0.17 $E_{1/2}$		-1.63 $E_{1/2}$	-2.37 E_{pc}	-2.54 E_{pc}	-2.66 $E_{1/2}$
Ph(dc)bpy		0.06 $E_{1/2}$		-1.95 $E_{1/2}$	-2.62 E_{pc}	-2.75 E_{pc}	
(MeO)Ph(7-CH ₃)bpy		0.06 $E_{1/2}$		-1.91 $E_{1/2}$	-2.62 E_{pc}	-2.74 E_{pc}	
(MeO)Ph(7-CF ₃)bpy		0.16 $E_{1/2}$		-1.63 $E_{1/2}$	-2.38 E_{pc}	-2.55 E_{pc}	-2.71 E_{pc}

^aPotentials in V and referenced versus the redox pair $\text{FeCp}_2/\text{FeCp}_2^+$. Cyclovoltammograms measured in 0.1 M $n\text{Bu}_4\text{NPF}_6$ /THF solution at ambient temperatures. Half-step potentials $E_{1/2}$, cathodic peak potentials E_{pc} , and anodic peak potentials E_{pa} . ^b from ref. [8].

Table S2. Absorption maxima of the protoligands Br-(R)Ph(R')bpy.^a

Protoligand	$\lambda_1 (\varepsilon_1)$	$\lambda_2 (\varepsilon_2)$	$\lambda_3 (\varepsilon_3)$	$\lambda_4 (\varepsilon_4)$
Br-Phbpy	286.4 (17.0)	227.0 (28.0)*		
Br-(MeO)Phbpy	296.8 (14.0)*	287.4 (16.7)	225.4 (25.5)*	
Br-Ph(6-{2-CH ₃ Ph})bpy	304.5 (9.6)*	279.6 (17.4)	245.5 (30.3)	
Br-Ph(6-{3-NO ₂ Ph})bpy	306.3 (11.3)*	272.9 (28.4)*	244.2 (48.5)	
Br-Ph(6-{3-MeOPh})bpy	299.2 (14.3)*	270.9 (23.7)*	248.8 (33.2)	
Br-Ph(6-{4-MeOPh})bpy	285.1 (35.9)	258.3 (27.2)		
Br-Ph(7-CH ₃)bpy	288.2 (12.2)	245.5 (15.7)*	224.1 (24.4)*	
Br-Ph(7-CF ₃)bpy	272.1 (18.4)	234.8 (23.8)*		
Br-Ph(dc)bpy	302.8 (11.8)*	293.9 (14.4)	245.4 (22.9)*	234.6 (26.7)*
Br-Ph(7-{3-MeOPh})bpy	289.8 (15.3)*	264.5 (18.4)		
Br-(MeO)Ph(7-CH ₃)bpy	289.2 (14.1)	227.8 (32.6)*		
Br-(MeO)Ph(7-CF ₃)bpy	292.9 (8.1)*	269.7 (15.1)	226.0 (32.4)*	

^a Measured in THF at rt. Absorption maxima λ in nm and extinction coefficients ε in $M^{-1} \text{cm}^{-1}$. * marks shoulders.

Table S3. Electrochemical data for the protoligands H-(R)Ph(R')bpy and Br-(R)Ph(R')bpy.^a

Protoligand	Red. I	Red. II	Red. III	Red. IV	Red. V
Br-(MeO)Phbpy		-2.63 E_{pc}	-2.71 $E_{1/2}$	-3.27 E_{pc}	
H-(MeO)Phbpy			-2.73 $E_{1/2}$	-3.27 E_{pc}	
Br-Ph(6-{2-CH ₃ Ph})bpy		-2.38 E_{pc}	-2.52 $E_{1/2}$		
Br-Ph(6-{3-NO ₂ Ph})bpy	-1.67 $E_{1/2}$	-2.70 E_{pc}	-2.76 $E_{1/2}$		
Br-Ph(6-{4-MeOPh})bpy		-2.54 E_{pc}	-2.64 $E_{1/2}$	-3.38 E_{pc}	
Br-Ph(6-{3-MeOPh})bpy		-2.51 E_{pc}	-2.54 $E_{1/2}$	-3.34 E_{pc}	
Br-Ph(7-CH ₃)bpy		-2.74 E_{pc}	-2.78 $E_{1/2}$	-3.26 E_{pc}	
Br-Ph(7-CF ₃)bpy		-2.46 E_{pc}	-2.62 E_{pc}	-2.82 $E_{1/2}$	
H-Ph(7-CF ₃)bpy			-2.57 E_{pc}	-2.76 $E_{1/2}$	-3.27 E_{pc}
Br-Ph(7-{3-MeOPh})bpy		-2.62 E_{pc}	-2.71 $E_{1/2}$	-3.18 E_{pc}	
Br-Ph(dc)bpy		-2.72 E_{pc}	-2.77 $E_{1/2}$	-3.29 E_{pc}	
Br-(MeO)Ph(7-CH ₃)bpy		-2.78 E_{pc}	-2.79 $E_{1/2}$		
Br-(MeO)Ph(7-CF ₃)bpy		-2.40 E_{pc}	-2.55 E_{pc}	-2.85 E_{pc}	
Br-PhTriazPy		-1.94 E_{pc}	-1.97 $E_{1/2}$	-2.87 E_{pc}	-3.16 E_{pc}
Br-(MeO)PhTriazPy		-1.88 E_{pc}	-1.93 $E_{1/2}$	-2.72 E_{pc}	-3.00 E_{pc}
H-(MeO)PhTriazPy			-1.97 $E_{1/2}$	-2.97 E_{pc}	-3.22 E_{pc}

^a Potentials in V and referenced versus the redox pair FeCp₂/FeCp₂⁺. Cyclovoltammograms measured in 0.1 M nBu₄NPF₆/THF solution at ambient temperatures. Half-step potentials $E_{1/2}$, cathodic peak potentials E_{pc} .

Table S4. Data from structure solution and refinement for complexes [Ni((MeO)Phbpy)Br], [Ni(Ph(7-{3-MeOPh})bpy)Br], and [Ni(Ph(6-{4-MeOPh})bpy)Br].

	[Ni((MeO)Phbpy)Br]	[Ni(Ph(7-{3-MeOPh})bpy)Br]	[Ni(Ph(6-{4-MeOPh})bpy)Br]
formula	C ₁₇ H ₁₃ BrN ₂ NiO	C ₂₃ H ₁₇ BrN ₂ NiO	C ₂₃ H ₁₇ BrN ₂ NiO
weight / g mol ⁻¹	399.91	476.00	476.00
temperature / K	170(2)	170(2)	170(2)
crystal system	triclinic	monoclinic	triclinic
space group	P $\bar{1}$	P 2 ₁ /c	P $\bar{1}$
cell parameters			
a / Å	8.9589(9)	14.004(2)	10.831(1)
b / Å	8.985(1)	9.5442(7)	17.080(1)
c / Å	9.189(1)	14.385(2)	17.292(1)
α / °	80.117(9)	90	63.026(7)
β / °	81.529(8)	102.23(1)	76.186(7)
γ / °	82.063(9)	90	79.082(7)
volume / Å ³	715.9(2)	1879.1(4)	2756.4(4)
Z	2	4	6
density, calc. / g cm ⁻³	1.855	1.683	1.721
F (000)	400	960	1440
total reflections	10708	34146	31455
unique reflections	3039	5080	11658
R _{int}	0.1640	0.5122	0.2809
R ₁ / wR ₂ [I ₀ >2σ(I)]	0.0530 / 0.0991	0.0670 / 0.1229	0.0542 / 0.0833
R ₁ / wR ₂ [all data]	0.1174 / 0.1230	0.2834 / 0.1954	0.2614 / 0.1293
goof on F ²	0.939	0.787	0.650
residual dens. / e·Å ⁻³	0.624 / -1.187	0.643 / -1.070	0.580 / -0.930
CCDC	1488104	1488106	1575607

Table S5. Data from structure solution and refinement for complexes $[\text{Ni}(\text{Ph}(7\text{-CF}_3)\text{bpy})\text{Br}]$ and $[\text{Ni}(\text{Ph}(6\text{-}\{2\text{-CH}_3\text{Ph}\})\text{bpy})\text{Br}]$.

	$[\text{Ni}(\text{Ph}(7\text{-CF}_3)\text{bpy})\text{Br}]$	$[\text{Ni}(\text{Ph}(6\text{-}\{2\text{-CH}_3\text{Ph}\})\text{bpy})\text{Br}]$
formula	$\text{C}_{17}\text{H}_{10}\text{BrF}_3\text{N}_2\text{Ni}$	$\text{C}_{23}\text{H}_{17}\text{BrN}_2\text{Ni}$
weight / g mol ⁻¹	437.89	460.00
temperature / K	170(2)	170(2)
crystal system	triclinic	monoclinic
space group	$P \bar{1}$	$P 2_1/c$
cell parameters		
a / Å	7.8525(7)	7.2434(9)
b / Å	8.6229(9)	9.6962(7)
c / Å	11.552(1)	25.645(3)
$\alpha / {}^\circ$	73.194(8)	90
$\beta / {}^\circ$	78.388(8)	94.643(9)
$\gamma / {}^\circ$	84.448(8)	90
volume / Å ³	732.9(1)	1795.2(3)
Z	2	4
density, calc. / g cm ⁻³	1.984	1.702
F (000)	432	928
total reflections	10794	18117
unique reflections	3938	3808
R _{int}	0.0995	0.2185
R ₁ / wR ₂ [I ₀ >2σ(I)]	0.0396 / 0.0583	0.0515 / 0.0915
R ₁ / wR ₂ [all data]	0.1204 / 0.0735	0.1533 / 0.1237
goof on F ²	0.820	0.819
residual dens. / e·Å ⁻³	0.568 / -0.986	0.626 / -1.474
CCDC	1501886	1582497

Table S6. Data from structure solution and refinement for compounds Br–PhTriazPy, Br–(MeO)PhTriazPy, H–(MeO)Phbpy, H–Ph(7-CF₃)bpy, and Br–Ph(7-CF₃)bpy.

	Br–PhTriazPy	Br–(MeO)PhTriazPy	H–(MeO)Phbpy	H–Ph(7-CF₃)bpy	Br–Ph(7-CF₃)bpy
formula	$\text{C}_{14}\text{H}_9\text{BrN}_4$	$\text{C}_{15}\text{H}_{11}\text{BrN}_4\text{O}$	$\text{C}_{17}\text{H}_{14}\text{N}_2\text{O}$	$\text{C}_{17}\text{H}_{11}\text{F}_3\text{N}_2$	$\text{C}_{17}\text{H}_{10}\text{BrF}_3\text{N}_2$
weight / g mol ⁻¹	313.16	343.19	262.30	300.28	379.18
crystal system	orthorhombic	orthorhombic	monoclinic	triclinic	monoclinic
space group	$P \text{na}2_1$	$P 2_12_12_1$	$P 2_1$	$P \bar{1}$	$P 2_1/n$
cell parameters					
a / Å	12.539(2)	6.6115(3)	10.514(2)	8.310(2)	11.1126(4)
b / Å	12.953(2)	11.8011(8)	5.3690(5)	10.937(3)	8.4616(3)
c / Å	7.6926(8)	17.822(1)	11.970(2)	16.987(5)	16.1630(7)
$\alpha / {}^\circ$	90	90	90	108.49(2)	90
$\beta / {}^\circ$	90	90	93.92(1)	101.10(2)	100.823(3)
$\gamma / {}^\circ$	90	90	90	92.45(2)	90
volume / Å ³	1249.5(3)	1390.5(1)	674.1(2)	1427.8(7)	1492.78(1)
Z	4	4	2	4	4
density, calc. / g cm ⁻³	1.665	1.639	1.292	1.397	1.687
F (000)	624	688	276	616	752
total reflections	22429	21061	13023	14088	41100
unique reflections	3207	2942	3604	6233	4043
R _{int}	0.1019	0.0780	0.2464	0.1151	0.0501
R ₁ / wR ₂ [I ₀ >2σ(I)]	0.0637 / 0.1580	0.0332 / 0.0676	0.0537 / 0.0935	0.0727 / 0.1873	0.0294 / 0.0722
R ₁ / wR ₂ [all data]	0.1197 / 0.1895	0.0564 / 0.0770	0.2907 / 0.1528	0.1926 / 0.2502	0.0434 / 0.0788
goof on F ²	1.065	1.043	0.713	0.967	1.063
residual / e·Å ⁻³	0.451 / -0.585	0.198 / -0.583	0.151 / -0.184	0.226 / -0.244	0.315 / -0.458
CCDC	1484146	1488102	1488108	1575606	1586570

Table S7. Comparison of selected DFT calculated and experimental structural data for complexes $[\text{Ni}(\text{Ph}(7\text{-CF}_3)\text{bpy})\text{Br}]$ and $[\text{Ni}(\text{Ph}(6\text{-}\{2\text{-CH}_3\text{Ph}\})\text{bpy})\text{Br}]$.

	$[\text{Ni}(\text{Ph}(7\text{-CF}_3)\text{bpy})\text{Br}]$		$[\text{Ni}(\text{Ph}(6\text{-}\{2\text{-CH}_3\text{Ph}\})\text{bpy})\text{Br}]$	
distances (\AA)	exp	calc	exp	calc
Ni–Br	2.2975(7)	2.317	2.300(1)	2.317
Ni–N1	1.855(3)	1.865	1.840(6)	1.861
Ni–C1	1.900(5)	1.918	1.905(8)	1.919
Ni–N2	1.962(4)	2.058	2.000(7)	2.0618
C1–C2	1.379(6)	1.401	1.40(1)	1.401
C1–C6	1.411(6)	1.430	1.42(1)	1.430
C6–C20	1.456(6)	1.457	1.46(1)	1.458
C24–C30	1.477(7)	1.467	1.45(1)	1.468
angles ($^\circ$)				
Br–Ni–N1	174.4(1)	178.4	178.5(2)	178.3
C1–Ni–N2	166.4(2)	164.7	165.6(3)	164.6
Br–Ni–C1	95.8(1)	97.7	96.9(2)	97.7
Br–Ni–N2	97.8(1)	97.6	97.4(2)	97.7
C1–Ni–N1	85.0(2)	83.9	83.7(3)	83.9
N1–Ni–N2	81.4(1)	80.8	81.9(2)	80.7
N1–C20–C6	111.8(4)	111.0	110.2(6)	111.0
N1–C24–C30	111.6(4)	114.0	113.1(6)	113.6
Ni–C1–C2	131.6(3)	130.1	131.4(6)	130.1
Ni–N2–C34	126.8(3)	128.4	129.4(5)	128.4
Ni–C1–C6	111.8(3)	112.5	112.8(6)	112.5
Ni–N2–C30	114.5(3)	112.6	112.5(5)	112.6
N2–C30–C24–C23	173.9(4)	179.8	177.9(7)	179.9
C1–C6–C20–C21	179.8(5)	180.0	173.5(7)	179.8

Table S8. Selected DFT calculated structural data for complexes $[\text{Ni}((\text{R})\text{Ph}(\text{R}')\text{bpy})\text{Br}]$.

	$\text{R} = \text{OMe}$	$\text{R}' = \text{CF}_3$	$\text{R}' = \text{CF}_3; \text{R} = \text{OMe}$
Ni–Br	2.319	2.312	2.313
Ni–N1	1.864	1.852	1.852
Ni–C1	1.916	1.903	1.902
Ni–N2	2.056	1.965	1.962
N2–Ni–C1	164.7	166.1	166.1
N1–Ni–Br	178.5	172.9	173.3
N2–Br–N1–C1	179.7	168.8	169.3
Tilt bpy	-	14.5	14.9

Table S9. DFT calculated low-energy transitions for $[\text{Ni}((\text{R})\text{Ph}(\text{R}')\text{bpy})\text{Br}]^a$

	$\lambda_{\text{max}} / \text{nm}$	$v_{\text{max}} / \text{cm}^{-1}$	f_{osc}
Phbpy	539.9	18522.6	0.00158
	536.3	18647.4	0.00119
	488.9	20452.0	0.00277
	465.8	21468.8	0.02158

(MeO)Phbpy	567.4	17625.2	0.00836
	538.3	18577.9	0.00103
	465.4	21486.3	0.00102
	467.1	21409.0	0.01525
Ph(7-CF ₃)bpy	548.8	18220.3	0.00145
	524.3	19072.4	0.00121
	500.3	19989.1	0.00761
	471.1	21227.9	0.00136

^aCalculated with TD-DFT; B3LYP-D3/TZVP/COSMO(THF).

Table S10. DFT ^a calculated low-energy transitions for [Ni(III)((MeO)Phbpy)Br]⁺⁺.

	λ_{\max} / nm	ν_{\max} / cm ⁻¹	f_{osc}
(1)	899.1	11122.2	0.01588
(2)	830.1	12046.2	0.10468
(3)	715.1	13983.2	0.01714
(4)	603.6	16567.4	0.00400
(5)	552.6	18095.4	0.00145
(6)	454.6	21996.5	0.00708

^aCalculated with TD-DFT; B3LYP-D3/TZVP/COSMO(THF).

Table S11. DFT calculated ^a EPR parameters for [Ni((R)Ph(R')bpy)Br]⁻.

	R = H	R = OMe	R' = CF ₃	R' = CF ₃ R = OMe
g_{iso}	2.0030	2.0032	2.0056	2.0056
	1.9930	1.9926	1.9883	1.9885
	2.0061	2.0061	2.0077	2.0075
	2.0101	2.0107	2.0208	2.0207
a(H)	-3.6/-10.5/-16.8	-3.6/-10.7/-17.0	-4.7/-11.9/-19.6	-4.8/-12.2/-20.0
a(H)	-4.4/-12.1/-19.3	-4.4/-12.2/-19.5	-4.7/-12.5/-20.1	-4.7/-12.6/-20.3
a(H)	-0.8/-5.8/-8.1	-0.7/-5.7/-7.9	0.7/3.0/5.5	0.8/3.0/5.6
a(H)	-1.1/-6.2/-8.8	-1.0/-6.1/-8.7	-1.0/-5.0/-5.9	-1.0/-5.2/-6.0
a(N)	-0.3/0.3/25.2	-0.2/0.4/25.3	1.5/2.0/25.8	1.5/2.0/25.8
a(N)	0.1/-0.1/26.9	-0.1/0.3/27.3	0.7/1.2/21.8	0.6/1.1/21.7

^a hyperfine coupling constants in MHz; level of theory: B3LYP-D3/TZVP/COSMO(THF)